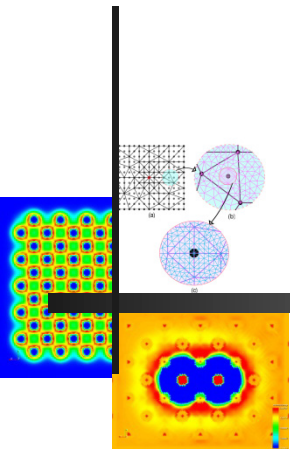


Electronic structure calculations at macroscopic scales



Vikram Gavini

*Department of Mechanical Engineering
University of Michigan, Ann Arbor*

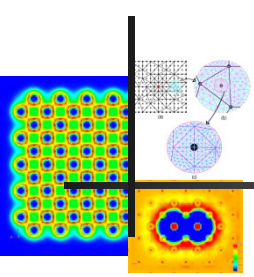
Collaborators:

B. Radhakrishnan (U. Michigan); P. Motamarri (U. Michigan); M. Iyer (U. Michigan); J. Knap (ARL); K. Bhattacharya (Caltech); M. Ortiz (Caltech)

Funding: NSF, AFOSR, ARO, XSESDE

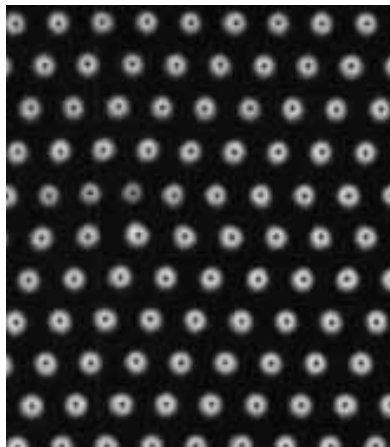


Defective Crystals



- Defects play a crucial role in influencing a variety of materials properties – mechanical, electronic, optical, chemical

- Dislocations

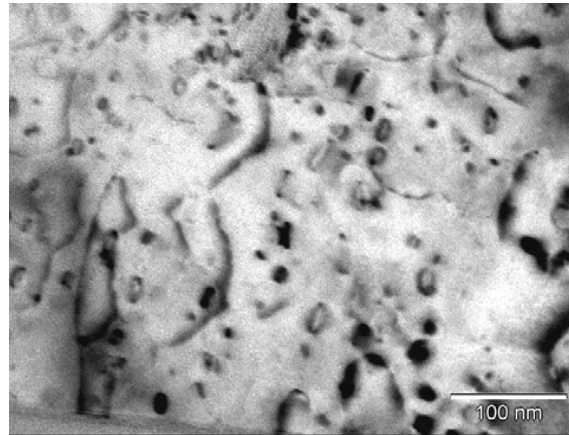


TEM image of dislocation partial
T.J. Balk, K.J. Hemker, Phil. Mag. A, 2001



Metal Plasticity –
Renders the strength of
materials to 1/1000 its
theoretical strength

Vacancies/Interstitials

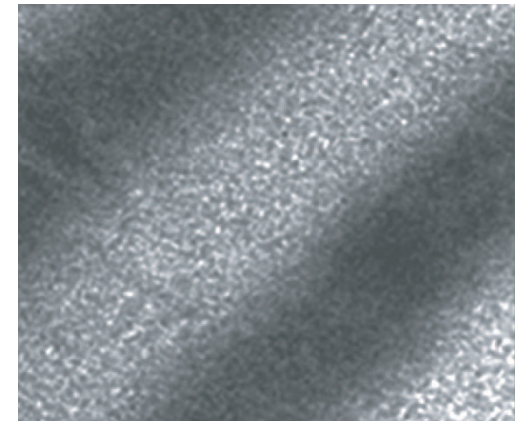


Prismatic loops formed from vacancies,
Giess et. al, Microsc Microanal, 2005



Creep, Spall, Ageing,
hardening due to radiation

Interfaces/Surfaces



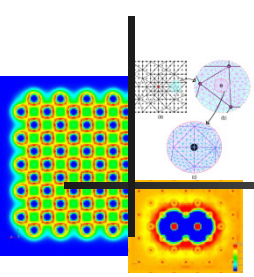
TEM image of Ni-Al interface,
Mann et.al, J. Appl. Phys. 1997



Phase stability, Energetics,
Diffusion mediation, defect
sources and sinks



Defective crystals: The challenge



- The energetics of defects: (i) core-energy; (ii) elastic energy
- The core of a defect is governed by electronic structure – need electronic structure calculations!
- Defects result in a vast span of *interacting* length scales
 - ❖ Electronic structure of the core (10^{-12} m)
 - ❖ Complex rearrangements of atoms around the core (10^{-9} m)
 - ❖ Long ranged elastic effects (10^{-6} m)

But need single physics
at all length scales! -
No patching, seamless
description

Realistic defect concentration in materials is parts per million!

- Challenge : Need electronic structure calculations at macroscopic scale!
(10^6 atoms and beyond)
- Idea: Systematic coarse-graining using adaptive numerical methods



Outline

- Motivation
- Background: electronic structure calculations
- *Orbital-free* density-functional theory (OFDFT)
- Quasi-continuum orbital-free density-functional theory (QC-OFDFT)
- Illustrative studies
 - ❖ Nucleation of prismatic dislocation loops
 - ❖ Nucleation of vacancies in shocks
 - ❖ Dislocation core studies
- Extensions to Kohn-Sham density functional theory (KSDFT)
- Concluding remarks



Quantum Mechanics

- Schrödinger equation - $H\psi = E\psi$

$$H = -\frac{1}{2} \sum_{i=1}^N \nabla_i^2 - \frac{1}{2} \sum_{A=1}^M \frac{1}{M_A} \nabla_A^2 - \sum_{i=1}^N \sum_{A=1}^M \frac{Z_A}{|\mathbf{r}_i - \mathbf{R}_A|} \\ + \sum_{i=1}^N \sum_{j>i}^N \frac{1}{|\mathbf{r}_i - \mathbf{r}_j|} + \sum_{A=1}^M \sum_{B=1, B>A}^M \frac{Z_A Z_B}{|\mathbf{R}_A - \mathbf{R}_B|}$$

$$\psi = \psi(\mathbf{x}_1, \mathbf{x}_2, \dots, \mathbf{x}_N, \mathbf{R}_1, \mathbf{R}_2, \dots, \mathbf{R}_M)$$

- Born-Oppenheimer approximation - Classical treatment of atomic nuclei

$$\psi = \psi(\mathbf{x}_1, \mathbf{x}_2, \dots, \mathbf{x}_N)$$

- Computational complexity - $\psi \in \mathbf{R}^{3N}$!!
-



Density-functional theory – Kohn-Sham approach

- Ground-state energy is a function of electron-density !! (Kohn & Sham, 1964-65)

$$\langle \psi | H | \psi \rangle \geq E_0 \quad (\text{Variational statement})$$

$$\begin{aligned} E_0 &= \min_{\psi} \langle \psi | T + \frac{1}{2} \sum_i \sum_j' \frac{1}{|\mathbf{r}_i - \mathbf{r}_j|} + \sum_i V_{ext}(\mathbf{r}_i) | \psi \rangle + E_{zz} \\ &= \min_{\psi} \langle \psi | T + \frac{1}{2} \sum_i \sum_j' \frac{1}{|\mathbf{r}_i - \mathbf{r}_j|} | \psi \rangle + \int \rho(\mathbf{r}) V_{ext}(\mathbf{r}) d\mathbf{r} + E_{zz} \\ &= \min_{\rho} \left\{ \underbrace{\left(\min_{\psi \rightarrow \rho} \langle \psi | T + \frac{1}{2} \sum_i \sum_j' \frac{1}{|\mathbf{r}_i - \mathbf{r}_j|} | \psi \rangle \right)}_{F(\rho)} + \int \rho(\mathbf{r}) V_{ext}(\mathbf{r}) d\mathbf{r} \right\} + E_{zz} \end{aligned}$$

$$F(\rho) = T_s(\rho) + E_H(\rho) + E_{xc}(\rho) \longrightarrow \begin{array}{l} \text{Exchange-correlation} \\ \text{functional: Model using} \\ \text{LDA, GGA} \end{array}$$

Kinetic energy of non-interacting electrons:
Computed from wave-functions of the
resulting E-L eqn.



Density-functional theory – *orbital-free* approach

➤ Model $T_s(\rho)$ \longrightarrow *Orbital-free* density-functional theory

➤ Thomas-Fermi (TF)

$$T_s(\rho) = \frac{3}{10}(3\pi^2)^{2/3} \int \rho^{5/3}(\mathbf{r}) d\mathbf{r} \quad (\text{Teller non-binding theorem})$$

➤ Thomas-Fermi-Weizsacker (TF- λ W)

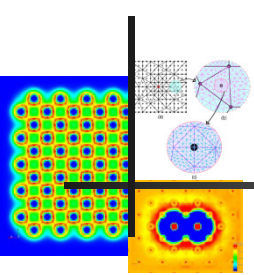
$$T_s(\rho) = \frac{3}{10}(3\pi^2)^{2/3} \int \rho^{5/3}(\mathbf{r}) d\mathbf{r} + \frac{\lambda}{8} \int \frac{|\nabla\rho(\mathbf{r})|^2}{\rho(\mathbf{r})} d\mathbf{r}$$

➤ Kernel-energies - subsequent improvement by Teter (1992), Smargiassi (1994), Carter (1998, 1999).

➤ *Orbital-free* density-functional theory is a good model for systems with electronic structure close to that of free-electron gas, e.g. aluminum, simple metals.



Orbital-free density-functional theory (OFDFT)



- The OFDFT energy functional is given by,

$$E(\rho, \mathbf{R}) = T_s(\rho) + E_{xc}(\rho) + E_H(\rho) + E_{ext}(\rho, \mathbf{R}) + E_{ZZ}(\mathbf{R})$$

$$T_s(\rho) = C_F \int \rho^{5/3}(\mathbf{r}) d\mathbf{r} + \frac{\lambda}{8} \int \frac{|\nabla \rho(\mathbf{r})|^2}{\rho(\mathbf{r})} d\mathbf{r} + T_k[\rho, \rho'; |\mathbf{r} - \mathbf{r}'|];$$

$$E_{xc}(\rho) = \int \epsilon_{xc}(\rho(\mathbf{r})) \rho(\mathbf{r}) d\mathbf{r}; \quad \text{Local density approximation (LDA)}$$

$$E_H(\rho) = \frac{1}{2} \int \int \frac{\rho(\mathbf{r}) \rho(\mathbf{r}')}{|\mathbf{r} - \mathbf{r}'|} d\mathbf{r} d\mathbf{r}';$$

$$E_{ext}(\rho, \mathbf{R}) = \int \rho(\mathbf{r}) V_{ext}(\mathbf{r}) d\mathbf{r}$$

$$= \sum_{I=1}^M \int \rho(\mathbf{r}) \frac{Z_I}{|\mathbf{r} - \mathbf{R}_I|} d\mathbf{r}$$

$$E_{zz}(\mathbf{R}) = \frac{1}{2} \sum_{I=1}^M \sum_{J=1, J \neq I}^M \frac{Z_I Z_J}{|\mathbf{R}_I - \mathbf{R}_J|};$$

Non-local

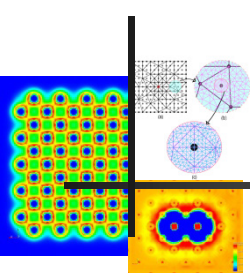
Classical electrostatic interaction energy :

Computed in Fourier-space (reciprocal-space) in almost all DFT implementations



OFDFT – Real-space formulation

(Gavini et al. JMPS 2007, 669-696)



Non-local

$$E_H(\rho) = \frac{1}{2} \int \int \frac{\rho(\mathbf{r})\rho(\mathbf{r}')}{|\mathbf{r} - \mathbf{r}'|} d\mathbf{r}d\mathbf{r}';$$

$$E_{ext}(\rho, \mathbf{R}) = \sum_{I=1}^M \int \frac{\rho(\mathbf{r})Z_I}{|\mathbf{r} - \mathbf{R}_I|} d\mathbf{r}; \quad \frac{1}{|\mathbf{r} - \mathbf{r}'|} \rightarrow \text{Green's function for Poisson's equation}$$

$$E_{zz}(\mathbf{R}) = \frac{1}{2} \sum_{I=1}^M \sum_{J=1, J \neq I}^M \frac{Z_I Z_J}{|\mathbf{R}_I - \mathbf{R}_J|};$$

- Electrostatic interactions can be re-written locally as,

$$E_H(\rho) + E_{ext}(\rho, \mathbf{R}) + E_{ZZ}(\mathbf{R}) = - \min_{\phi} \left\{ \frac{1}{8\pi} \int |\nabla\phi(\mathbf{r})|^2 d\mathbf{r} - \int (\rho(\mathbf{r}) + b(\mathbf{r}; \mathbf{R}))\phi(\mathbf{r}) d\mathbf{r} \right\}$$

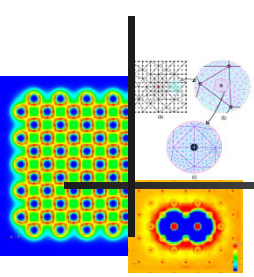
↓
(Regularized nuclear charges)

- Thus, $E(\rho, \mathbf{R}) = \max_{\phi} L(\phi, \rho, \mathbf{R})$

$$L(\phi, \rho, \mathbf{R}) = C_F \int \rho^{5/3}(\mathbf{r}) d\mathbf{r} + \frac{\lambda}{8} \int \frac{|\nabla\rho(\mathbf{r})|^2}{\rho(\mathbf{r})} d\mathbf{r} + \int \epsilon_{xc}(\rho(\mathbf{r}))\rho(\mathbf{r}) d\mathbf{r} - \frac{1}{8\pi} \int |\nabla\phi(\mathbf{r})|^2 d\mathbf{r} + \int (\rho(\mathbf{r}) + b(\mathbf{r}))\phi(\mathbf{r}) d\mathbf{r}$$



OFDFT – Real-space formulation



- To enforce constraint, $\rho > 0$, make substitution, $\rho = u^2$
- The problem of computing the ground state energy is given by saddle-point problem is given by,

$$\min_{\mathbf{R}} \min_u \max_{\phi} L(\phi, u, \mathbf{R}) \quad \text{subject to: } \int u^2(\mathbf{r}) d\mathbf{r} = N$$

$$L(\phi, u, \mathbf{R}) = \frac{\lambda}{2} \int |\nabla u(\mathbf{r})|^2 d\mathbf{r} + C_F \int u^{10/3}(\mathbf{r}) d\mathbf{r} + \int \varepsilon_{xc}(u^2(\mathbf{r})) u^2(\mathbf{r}) d\mathbf{r} \\ - \frac{1}{8\pi} \int |\nabla \phi(\mathbf{r})|^2 d\mathbf{r} + \int (u^2(\mathbf{r}) + b(\mathbf{r}; \mathbf{R})) \phi(\mathbf{r}) d\mathbf{r}$$

- The ground-state energy and electron-density is expressed as a variational saddle-point problem in real-space with a **local** functional that is amenable to computation.

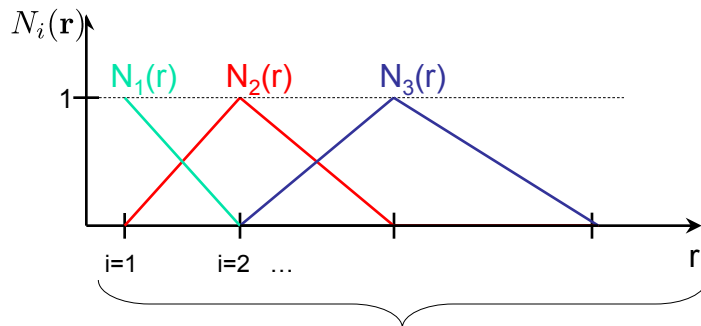
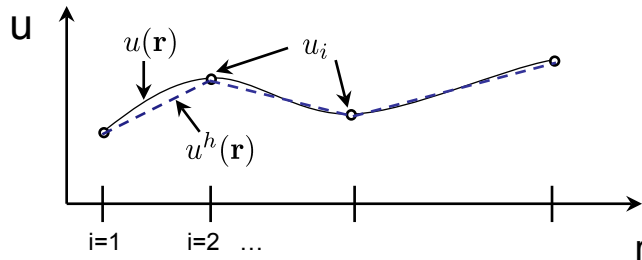


OFDFT – FE discretization

- Use finite-element basis for computing –

$$u^h(\mathbf{r}) = \sum_i u_i N_i(\mathbf{r}), \quad \phi^h(\mathbf{r}) = \sum_i \phi_i N_i(\mathbf{r})$$

u_i, ϕ_i – Nodal values
 $N_i(\mathbf{r})$ – Shape functions



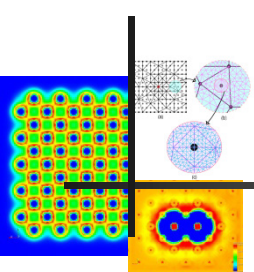
By changing the positioning of the nodes the spatial resolution of basis can be changed/adapted

Features of finite-element basis:

1. FE basis are local, and their spatial resolution can be changed/adapted.
2. Complex geometries can be represented, and arbitrary boundary conditions can be imposed.
3. There is a systematic way of controlling the smoothness of the basis functions, from linear functions to any higher degree polynomial.
4. The local nature of the basis enables parallel implementation of the numerical scheme with ease.



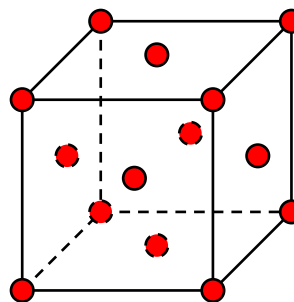
Illustrative examples – Aluminum nano-clusters



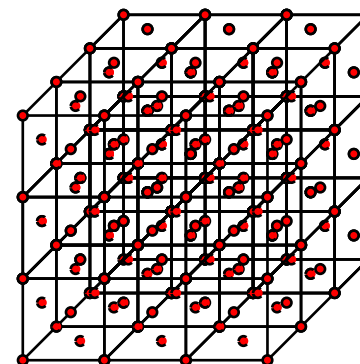
- Need a real-space formulation.
- TFW KE functionals, LDA appx. for exchange correlation functionals.
- Goodwin-Needs-Heine pseudo-potential for Aluminum
- Simulations are performed on a range of cluster sizes

1x1x1
3x3x3
5x5x5
9x9x9

} FCC unit cells



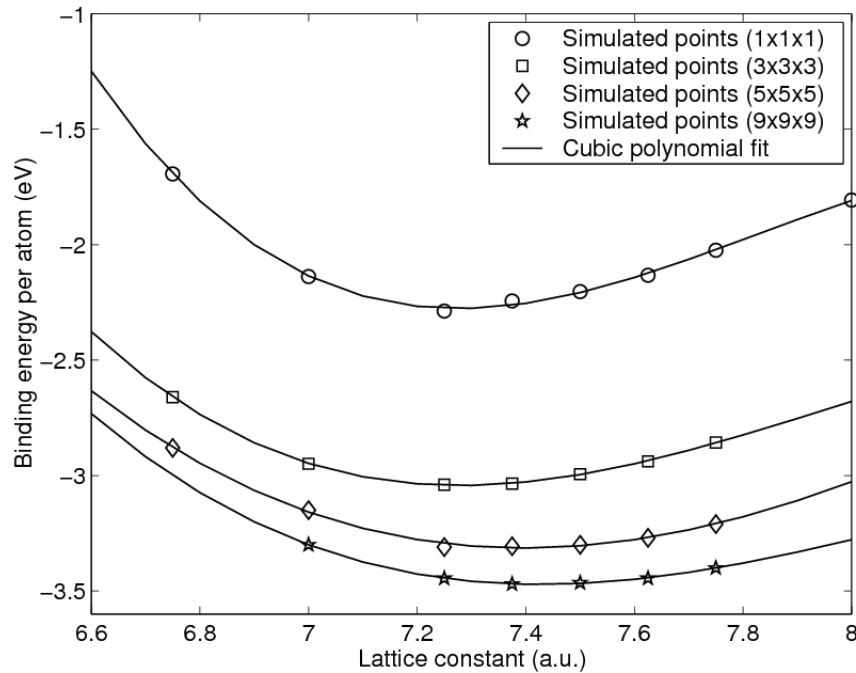
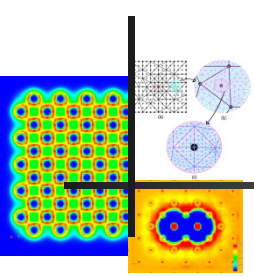
1x1x1 fcc cluster



3x3x3 fcc cluster



Results – Aluminum clusters



Binding energy per atom as a function of lattice constant

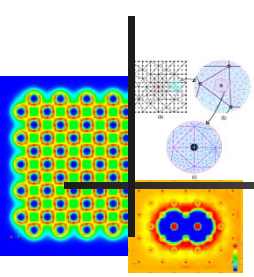
Property	OFDFT-FE	KS-LDA ^a	Experiments ^b
Lattice parameter (a.u.)	7.42	7.48	7.67
Cohesive energy (eV)	3.69	3.67	3.4
Bulk modulus (GPa)	83.1	79.0	74.0

a Goodwin et al. (1990), Gaudion et al. (2002)

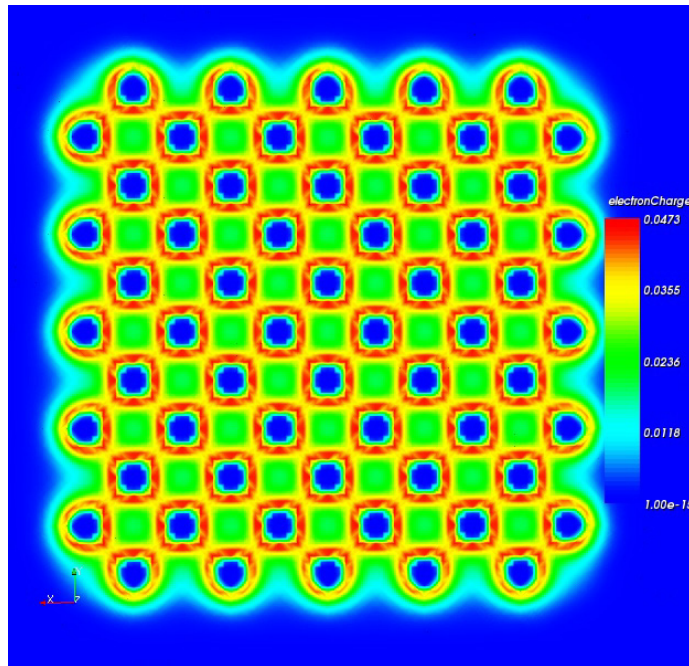
b Brewer (1997), Gschneider (1964)



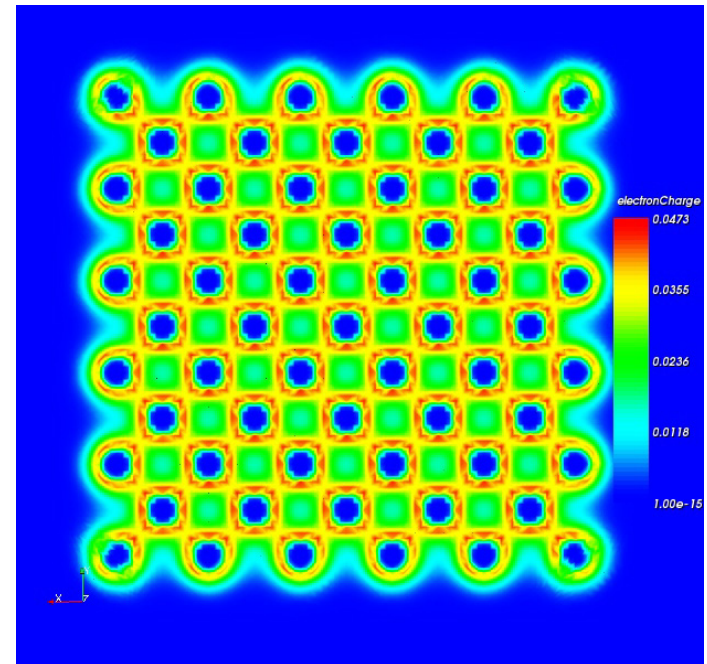
Results – Aluminum clusters



Contours of electron-density in an aluminum cluster
with 5x5x5 fcc unit cells (666 atoms)



Mid-plane



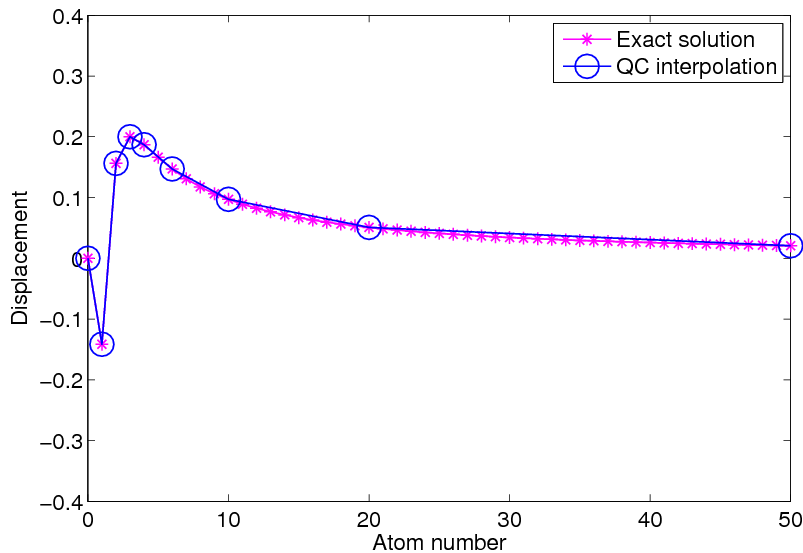
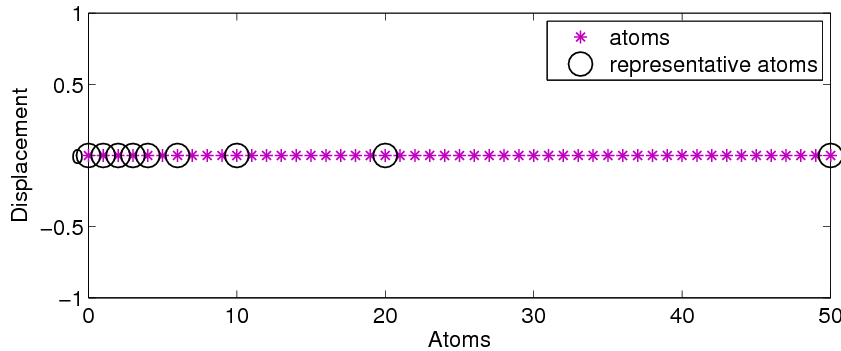
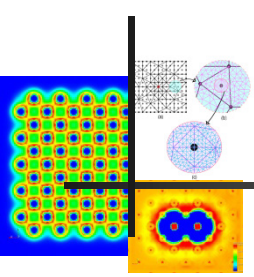
Face

3,000,000 elements; 3000 CPU hours !!

Need coarse-graining!



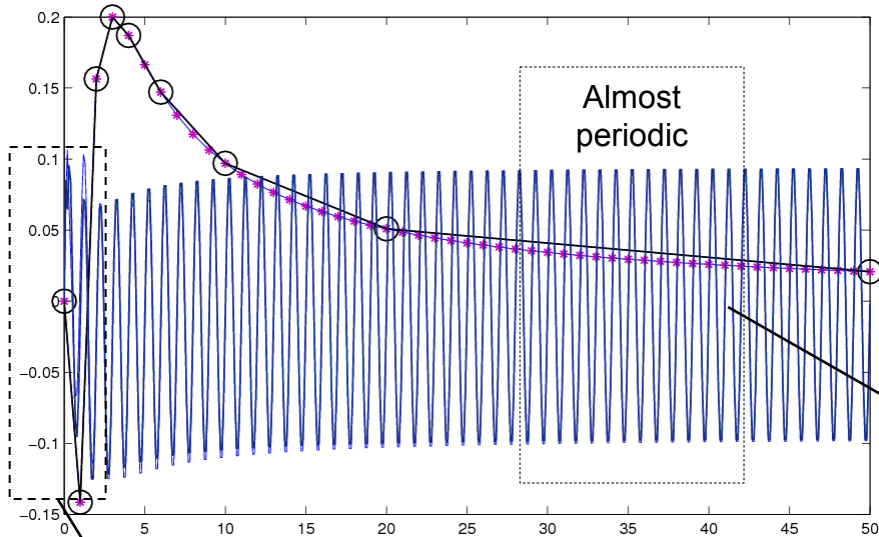
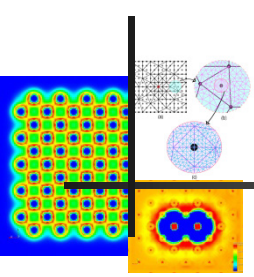
Theory of Quasi-Continuum (Tadmor et al. 1995, Knap & Ortiz 2003)



- Seamless multi-scale scheme to transition from atomistics to continuum.
- Main Features of QC:
 - ❖ Kinematically constraint atoms to finite-element mesh.
 - ❖ Adaptive mesh refinement
 - ❖ Cluster summation rules.
- Developed in the context of lattice atomistics.
- Extension to electronic structure calculations pose challenges!



Coarse-graining of OFDFT : Challenge



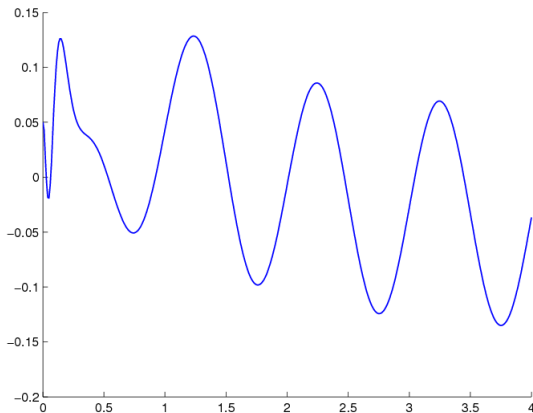
- Subatomic oscillations and lattice scale modulations of electron density and electrostatic potential !!
- For slowly varying deformation fields, the energy can be written as (Blanc et al. 2002),

$$\mathcal{E}(\mathbf{x}) = \int W_{Per}^{TFW}(\mathbf{F}) d\Omega$$

↓
Periodic unit cell
calculation

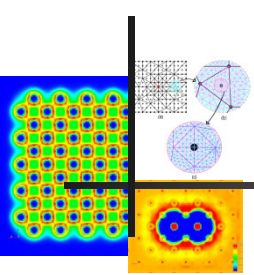
Exploit this fact in big elements while retaining full resolution in small elements.

Far from periodic close to the defect



Quasi-Continuum OFDFT (QC-OFDFT) – Key Ideas

(Gavini et al. JMPS 2007, 697-718)

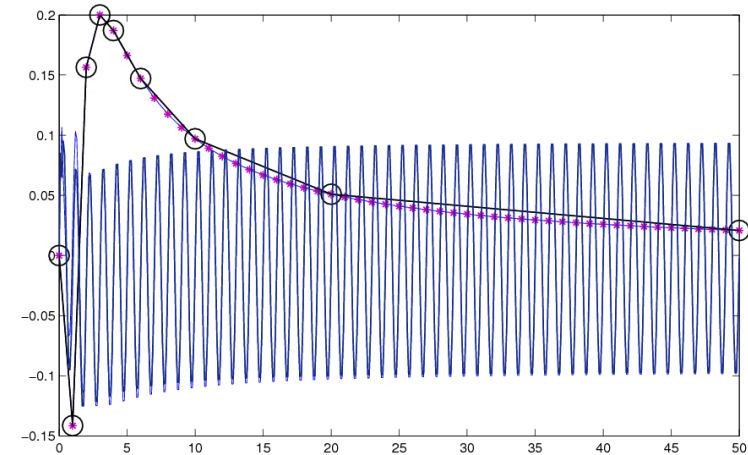


- Constrain atomic positions following an adaptive supra-atomic mesh (T_{h1})
- Write electronic fields as a sum of two terms

$$\begin{aligned}\phi^h &= \phi_0^h + \phi_c^h, \\ u^h &= u_0^h + u_c^h\end{aligned}$$

- Predictor u_0^h, ϕ_0^h

Computed element by element assuming periodicity on a local sub-atomic mesh



- Corrector u_c^h, ϕ_c^h

Computed on an adaptive mesh which is sub-atomic near defects and coarsens away from it (T_{h3})

$$\min_{u_c^h} \max_{\phi_c^h} L(\phi_0^h + \phi_c^h, u_0^h + u_c^h, \mathbf{R})$$



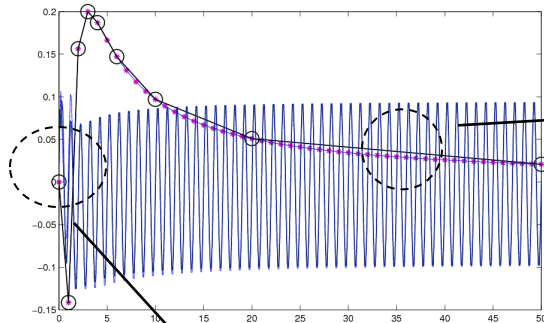
QC-OFDFT – Key Ideas

- We introduce cluster quadrature rules for an element e in T_{h_3} ,

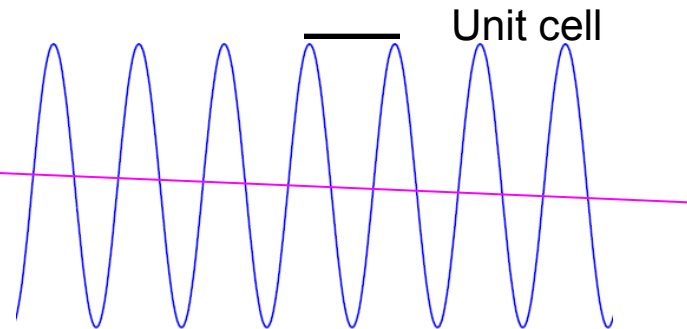
$$\int_e f(\mathbf{r}) d\mathbf{r} \approx |e| \langle f \rangle_{D_e}$$

$|e|$ is the volume of the element, D_e is the unit cell of an atom if such a cell is contained in e or e otherwise and $\langle f \rangle_{D_e}$ is the average of f over D_e .

- *Philosophy behind cluster quadrature rules:*



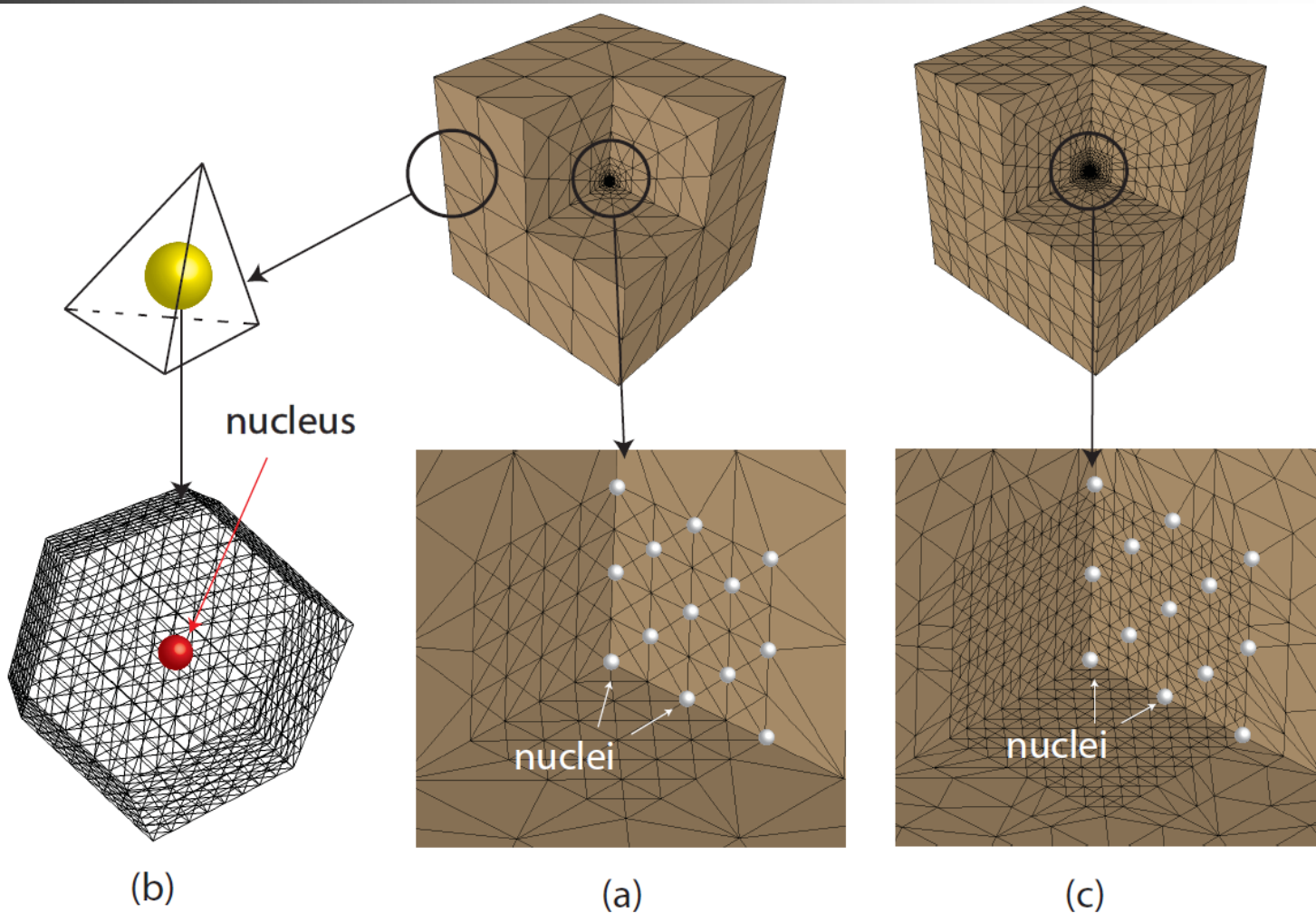
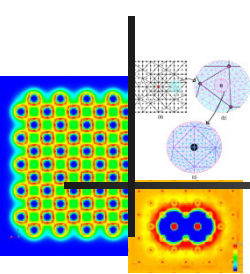
Exact integration required



Integration on unit cell –
zero order quadrature rule



QC-OFDFT – Meshes



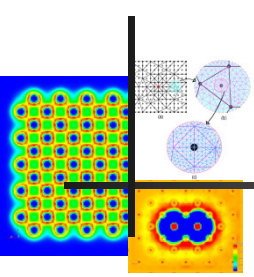
Mesh used to compute the predictor fields

Mesh used to compute the nuclear positions

Mesh used to compute the corrector fields



QC-OFDFT – Properties

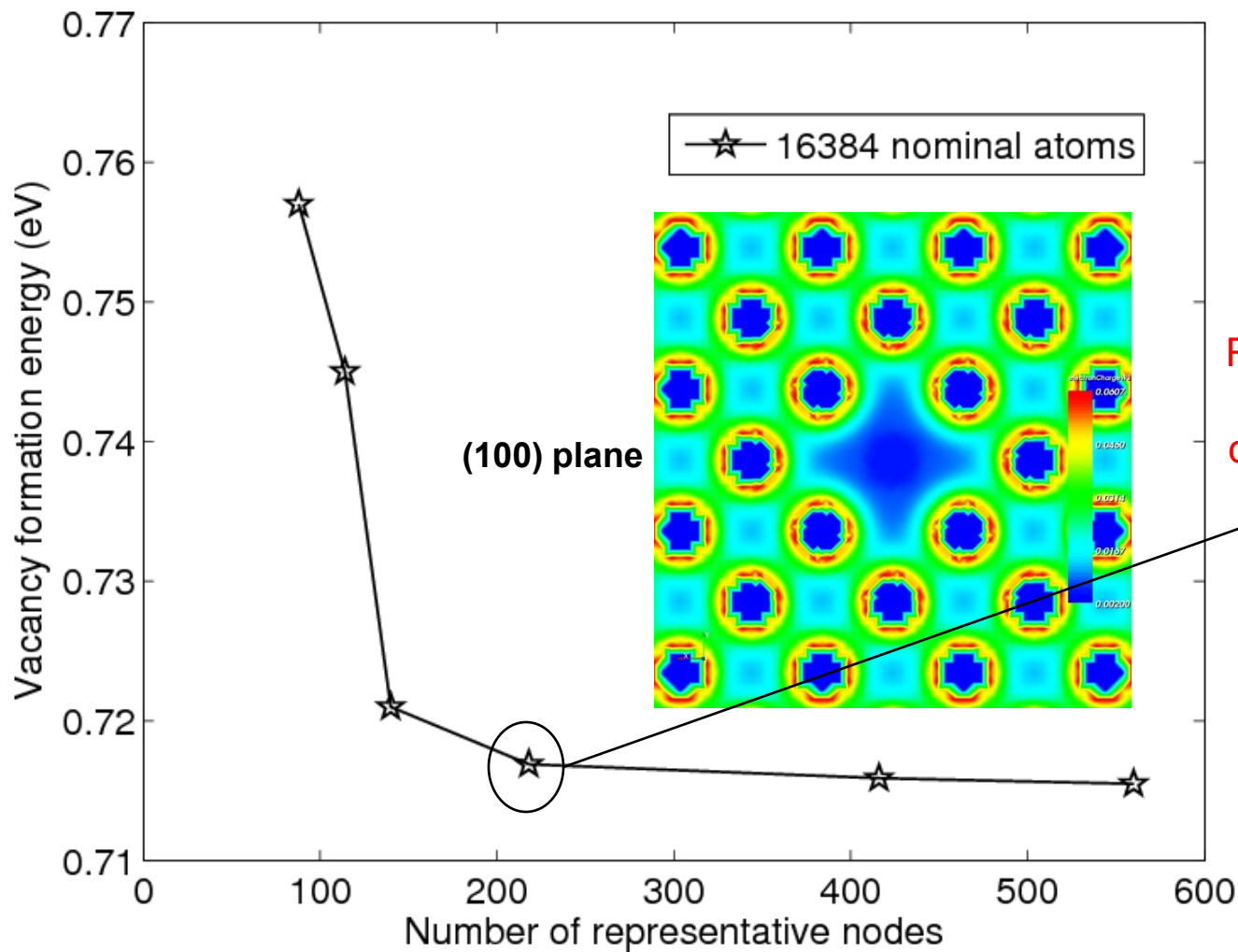


The proposed approximation scheme (QC-OFDFT) has the following properties:

- adapts the level of spatial resolution to the local structure of the solution;
- coarse-graining is completely **unstructured and seamless**;
- fully-resolved OFDFT and finite lattice-elasticity are obtained as extreme limits;
- OFDFT is the **sole physics** input to the calculations, and no spurious physics or ansatz regarding the behavior of the system is introduced;
- a converged solution obtained by this scheme may be regarded as a solution of OFDFT;
- **million atom OFDFT calculations possible at no significant loss of accuracy!!**



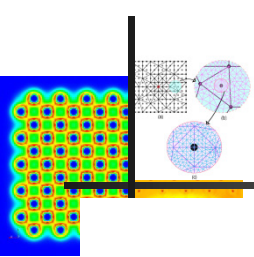
Vacancy in aluminum: Convergence of QC approximation



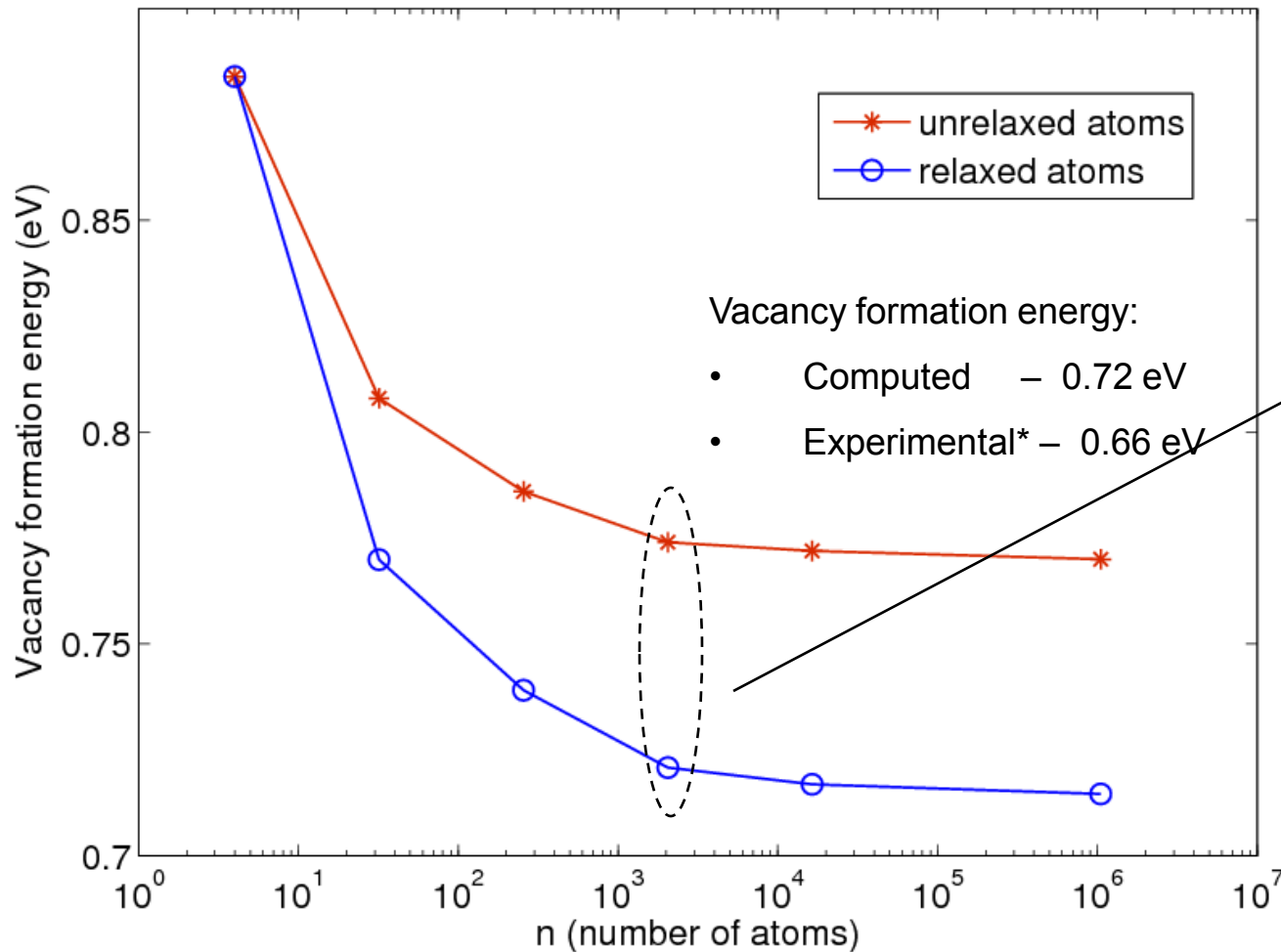
16,384 atoms in the computational cell

Reached convergence. Almost 80 fold computational savings!





Vacancy in Aluminum: Convergence with cell-size



Vacancy formation energy:

- Computed – 0.72 eV
- Experimental* – 0.66 eV

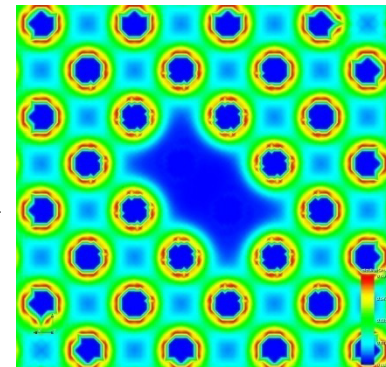
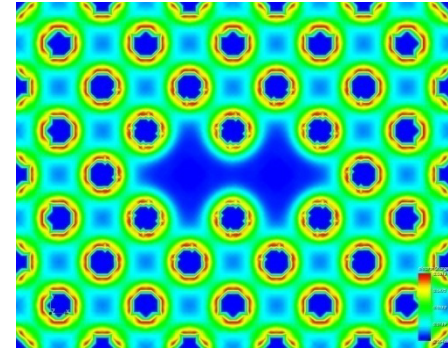
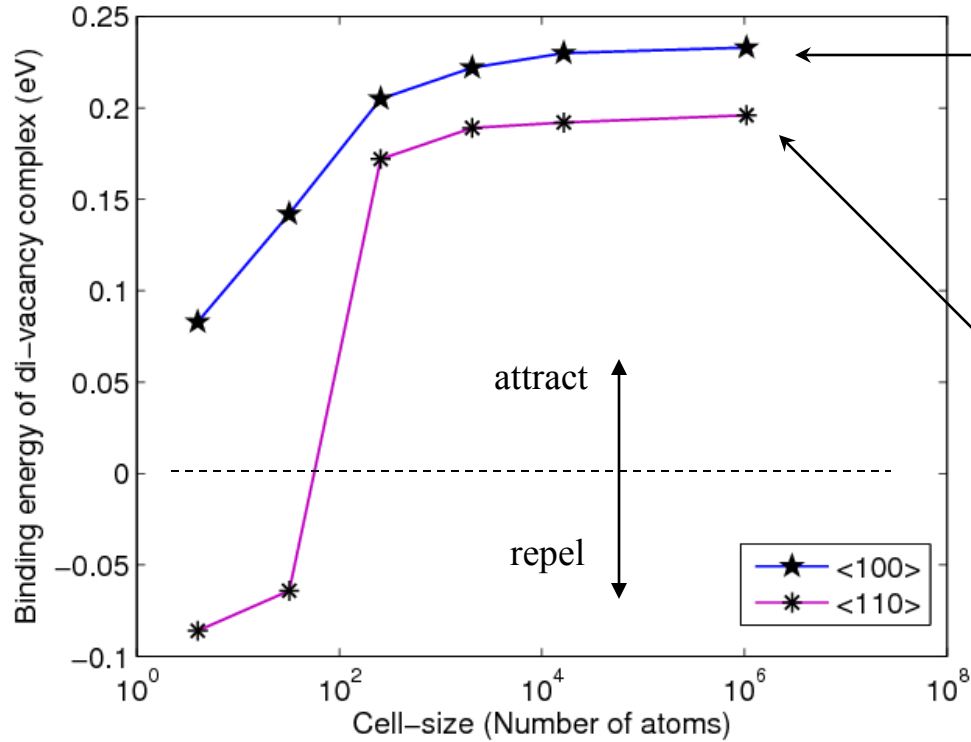
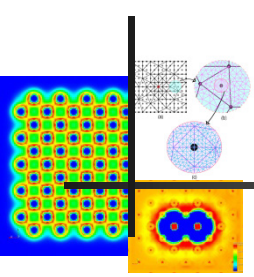
Need almost 1000 atoms for convergence w.r.t to cell-size!

Long-ranged effects in defects

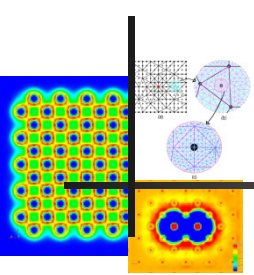
* Triftshauer 1975



Di-vacancy binding energy – cell-size effect



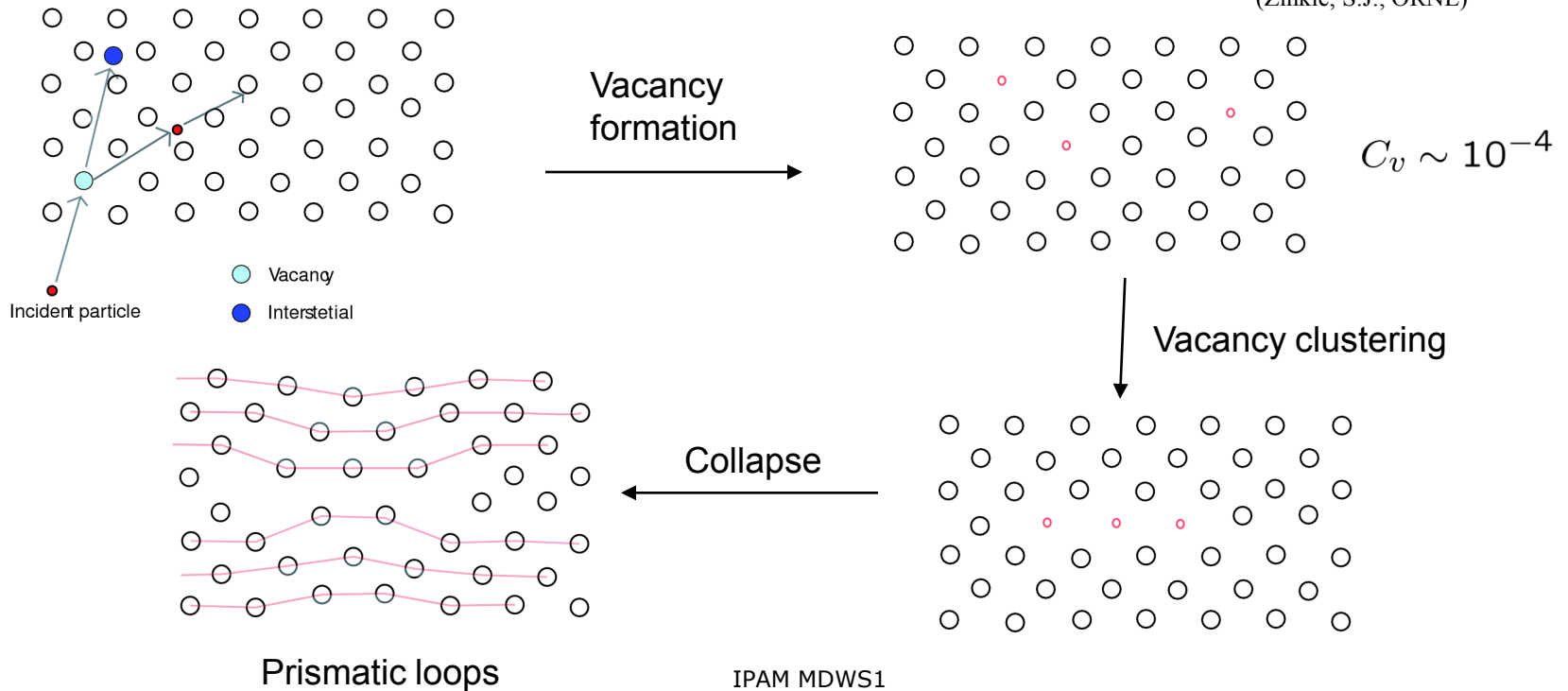
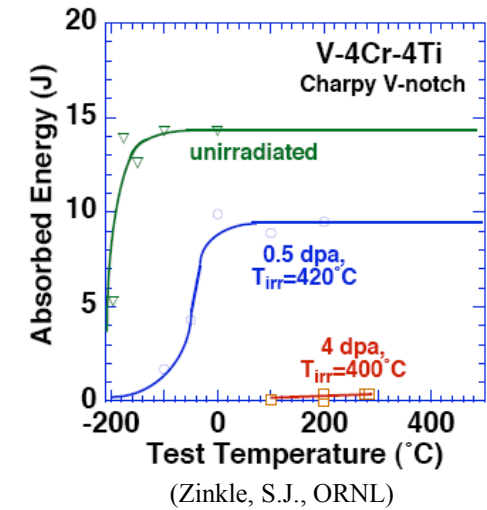
Radiation Damage



Effects of radiation on material properties :

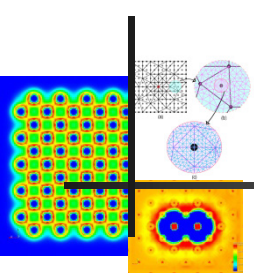
- ❖ Reduced fracture toughness; Increased hardness
- ❖ Material swelling

Mechanism behind radiation damage (Hypothesis):



Vacancy clustering in aluminum

(Gavini et al. PRB 2007, 76 180101(R))



➤ Quad-vacancies formed from two di-vacancies

	Structure	Positions of vacancies	Vacancy binding energy (eV)
1	planar {100}	(0,0,0), (a/2,a/2,0), (a,0,0), (a/2,-a/2,0)	0.52
2	planar {100}	(0,0,0), (a/2,a/2,0), (a,0,0), (3a/2,a/2,0)	0.50
3	planar {100}	(0,0,0), (a/2,a/2,0), (a,0,0), (a,a,0)	0.48
4	planar {100}	(0,0,0), (a,0,0), (0,a,0), (a,a,0)	0.48
5	planar {110}	(0,0,0), (0,a/2,a/2), (a,0,0), (a,a/2,a/2)	0.56
6	planar {111}	(0,0,0), (0,a/2,a/2), (a/2,a/2,0), (a/2,a,a/2)	0.55
7	non-planar	(0,0,0), (0,a/2,a/2), (a/2,0,a/2), (a/2,a/2,0)	0.53
8	non-planar	(0,0,0), (a,0,0), (a/2,a/2,0), (a/2,0,a/2)	0.51
9	non-planar	(0,0,0), (a,0,0), (a/2,a/2,0), (0,a/2,a/2)	0.50

➤ Larger clusters

- ❖ {110} plane
- ❖ 6 vacancy rectangular cluster : Binding energy = 0.81eV
- ❖ 9 vacancy rectangular cluster : Binding energy = 1.16eV
- ❖ {111} plane
- ❖ 7 vacancy hexagonal cluster : Binding energy = 0.88eV

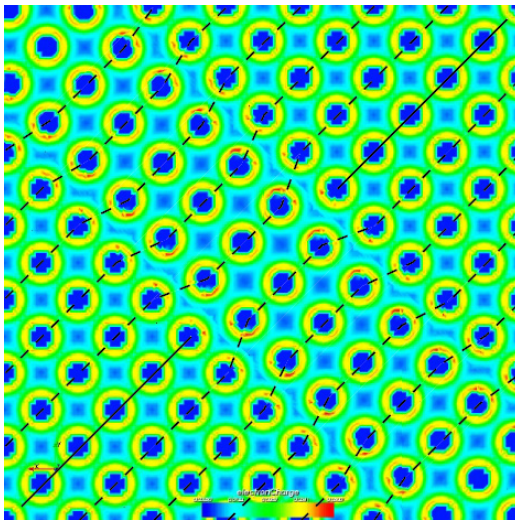
Growth of clusters appears energetically favorable!



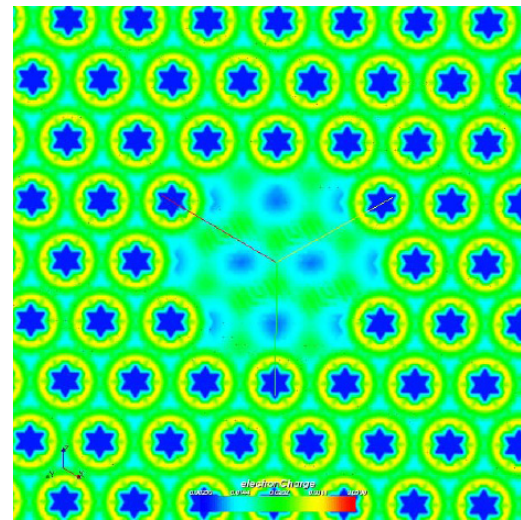
Prismatic loop nucleation

➤ $\{111\}$ plane - 7 vacancy hexagonal cluster

- Binding energy = 0.88 eV (non-collapsed)
- Binding energy = 1.55 eV (collapsed – prismatic loop)



(001)



(111)

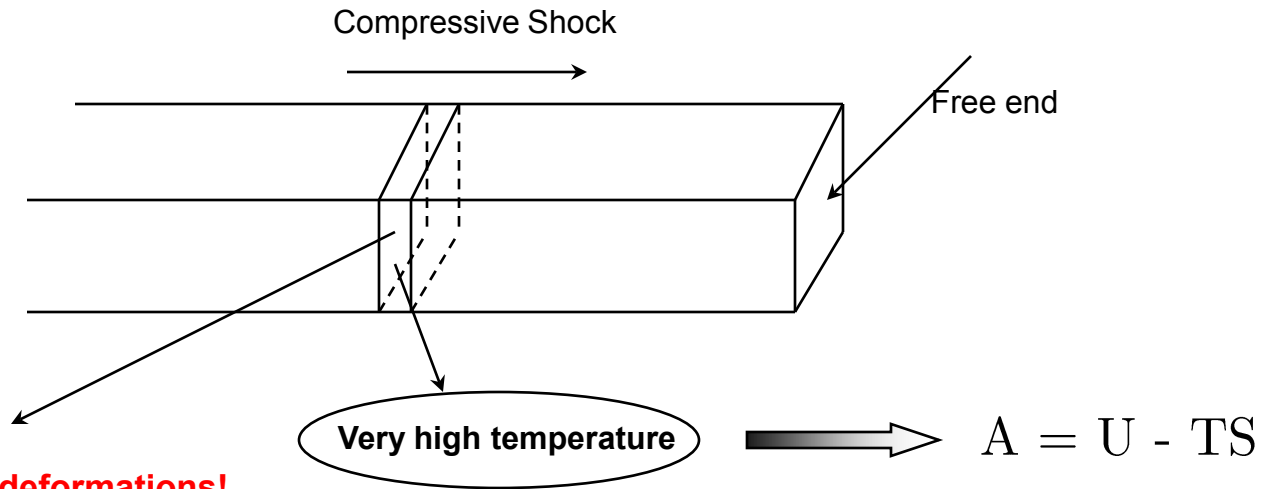
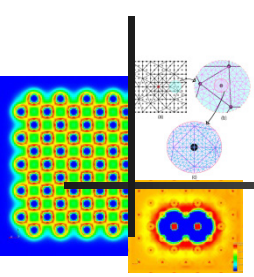
$1/2\langle 110 \rangle$ Vacancy prismatic loop

Cell-size	Binding energy (collapsed loop)
16,384	0.91 eV
1,048,576	1.55 eV

Stability observed only at multi-million atoms!

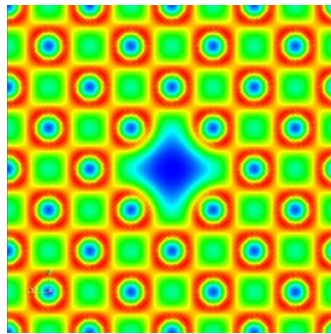


Dynamic Fracture -- Spalling

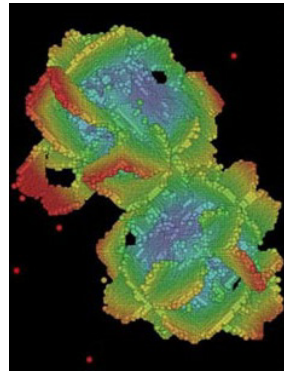


Also, extreme deformations!

$U(F)?$



Vacancy nucleation



Void formation and coalescence

(Seppala et al, 2005)

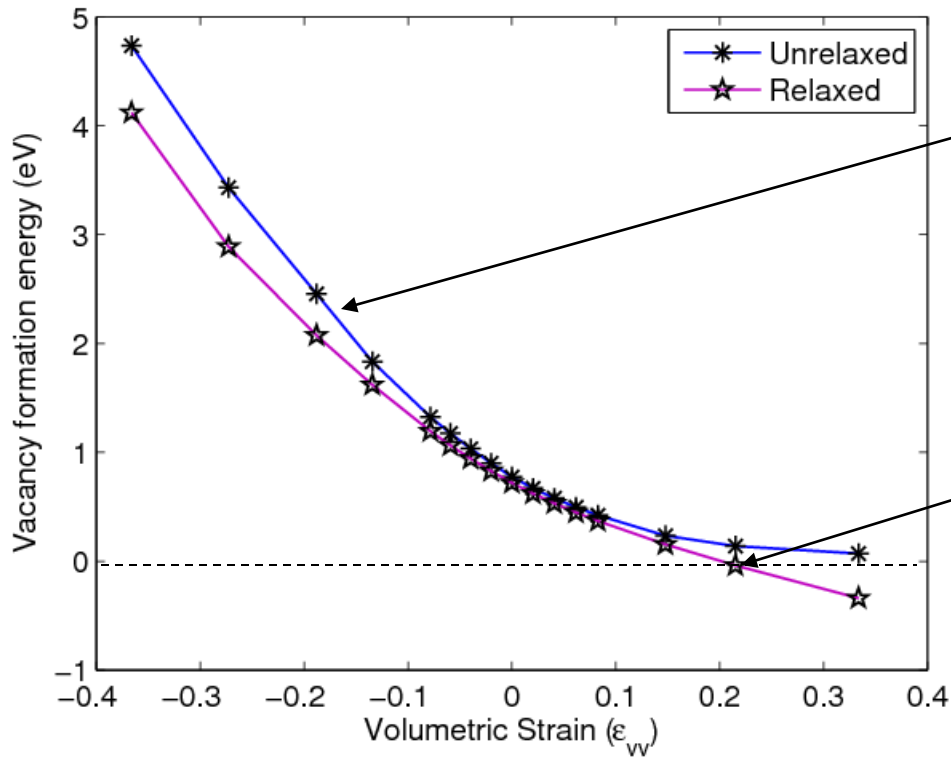
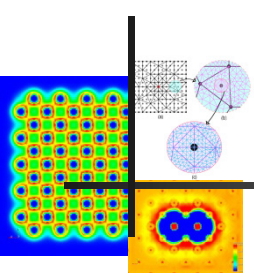


Spall fracture



Importance of the defect-core in the energetics of defects

(Gavini, Phys. Rev. Lett 2008, **101** 205503; Gavini, Proc. Roy. Soc. **465** 3239)



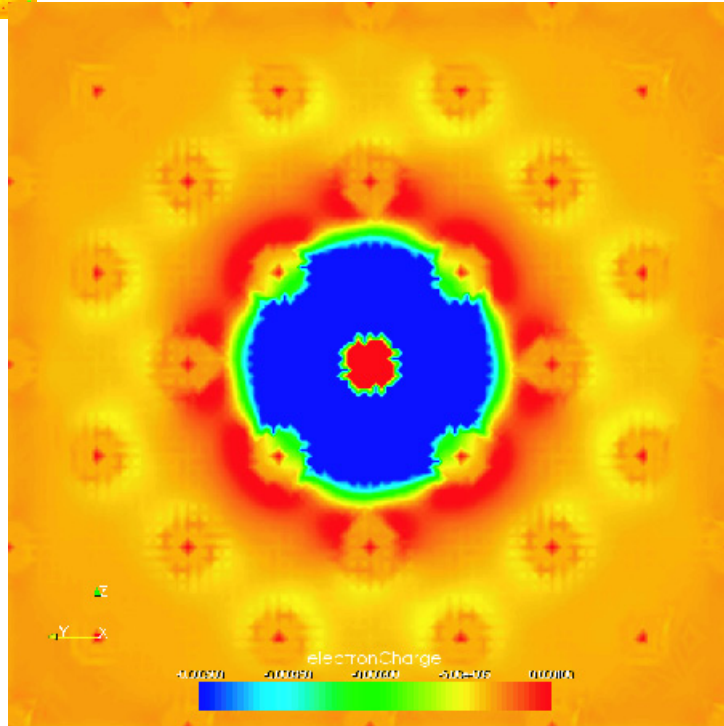
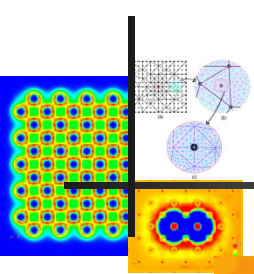
Electronic structure of the core significantly influenced by macroscopic deformations.

Core energy not an inconsequential constant!

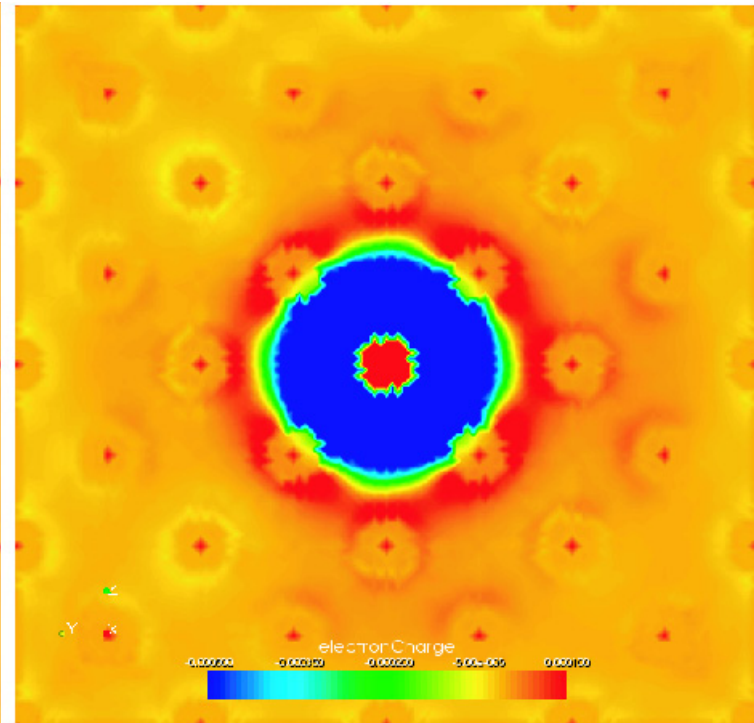
Vacancies become thermodynamically favorable! Spontaneous nucleation of vacancies!



Changing nature of the defect core



No volumetric strain



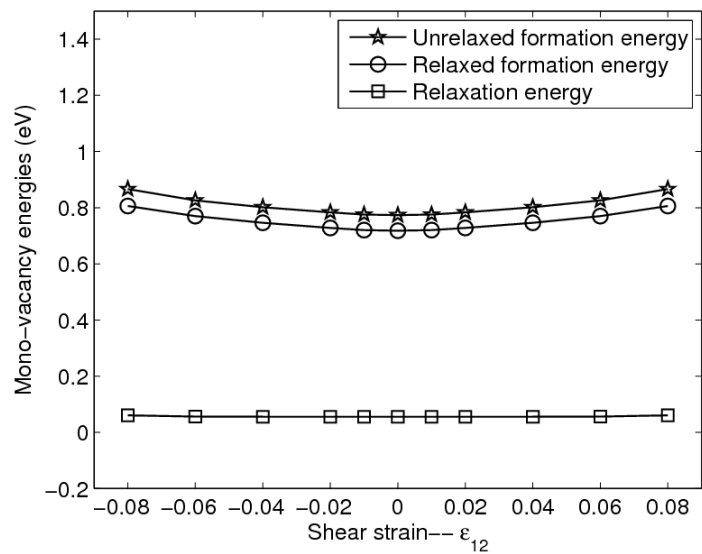
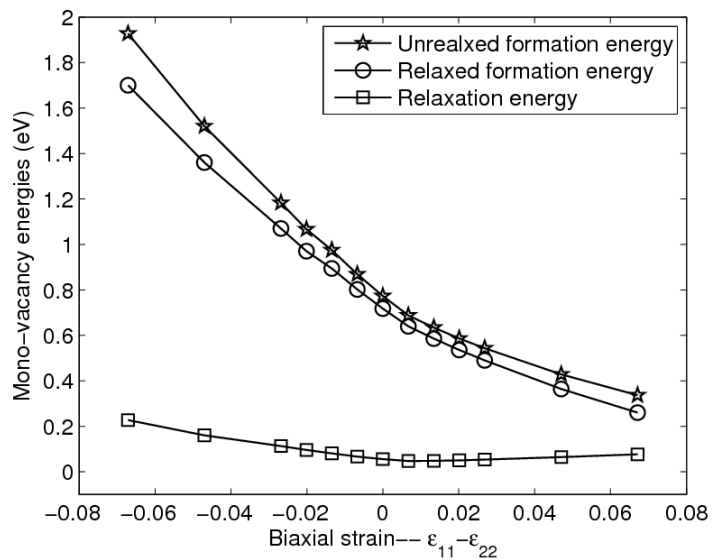
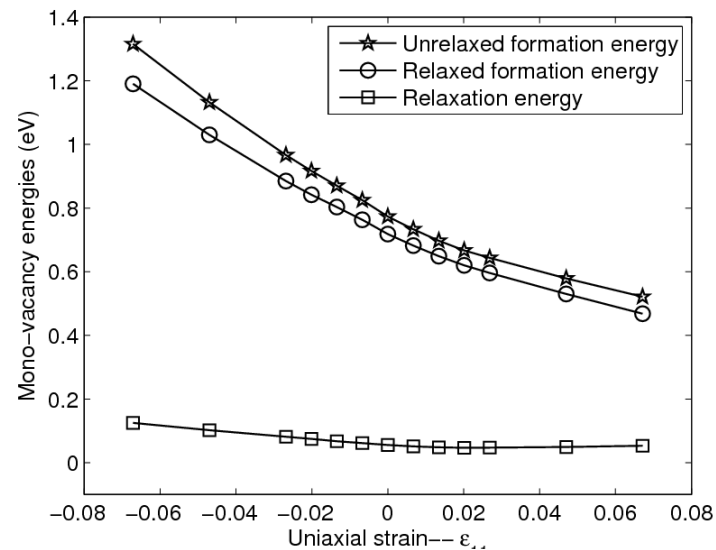
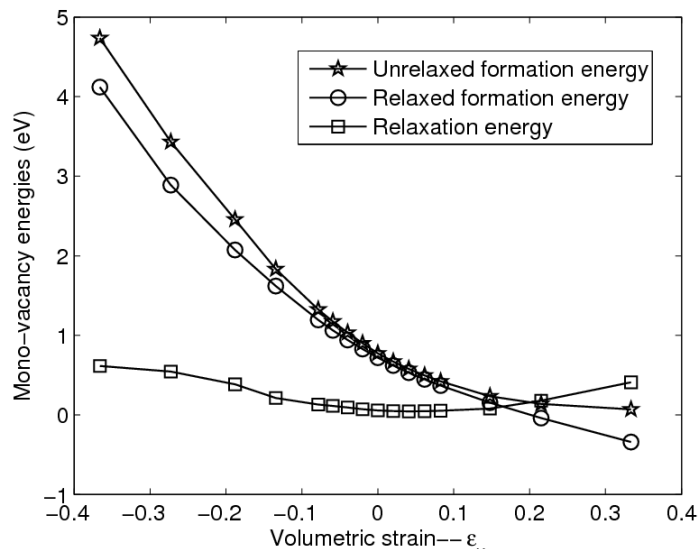
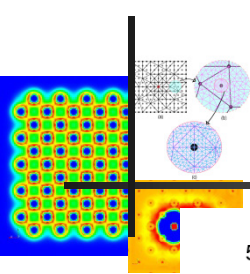
0.3 volumetric strain

The nature of the displacement fields also change with volumetric strain:

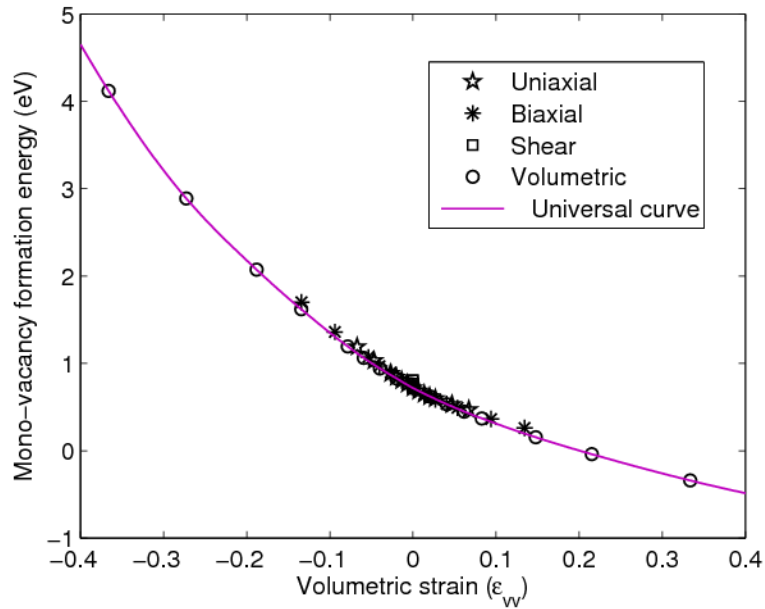
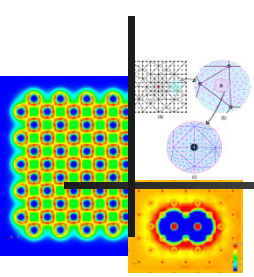
- Maximum displacement 0.17 a.u. **inwards** for -0.3 volumetric strain
- Maximum displacement 0.03 a.u. **inwards** for zero volumetric strain
- Maximum displacement 0.19 a.u. **outwards** for 0.3 volumetric strain



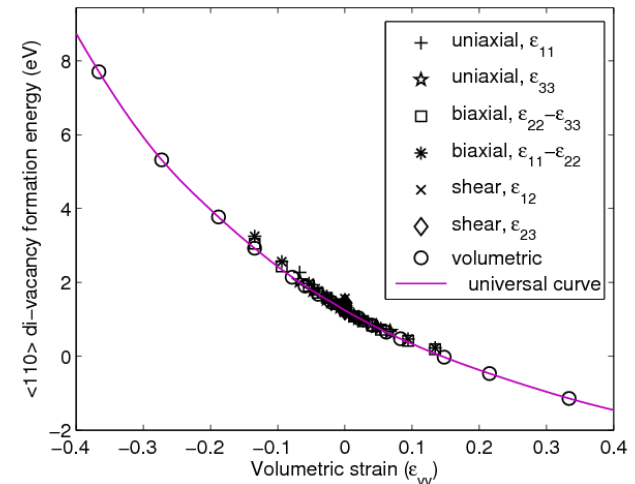
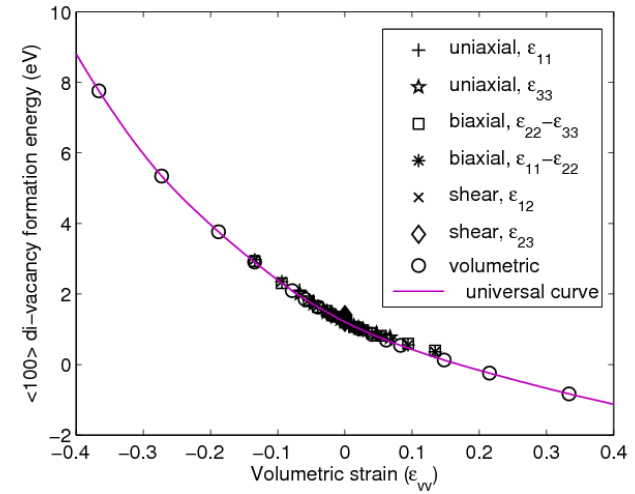
Role of macroscopic deformations on energetics of vacancies



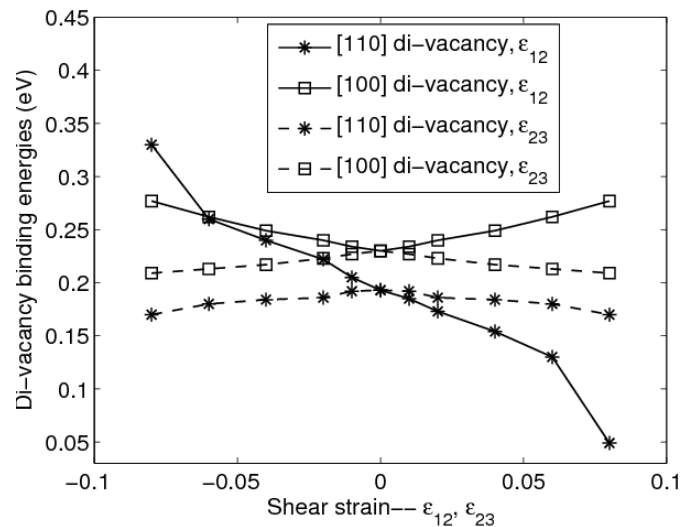
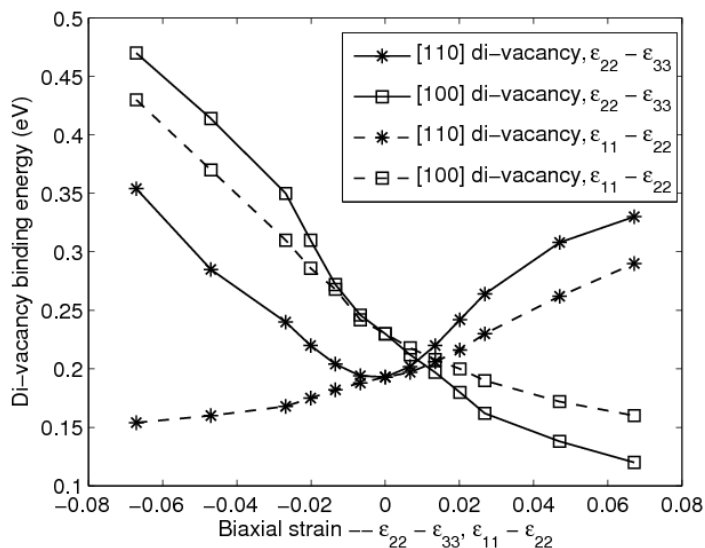
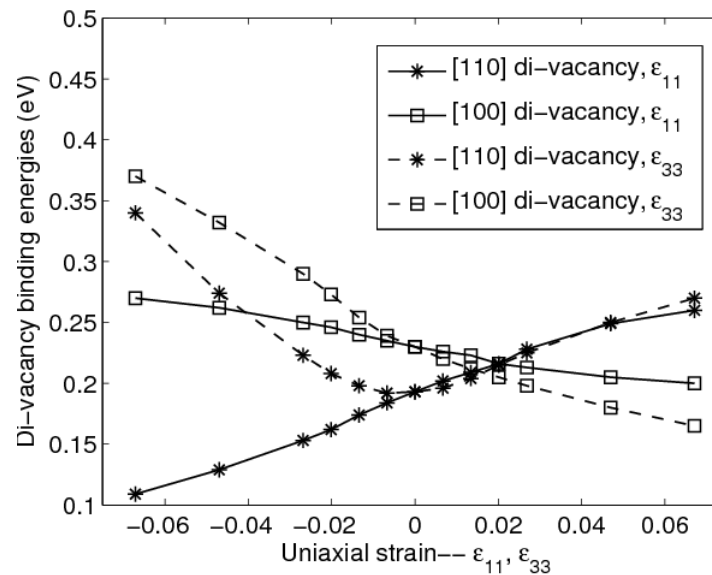
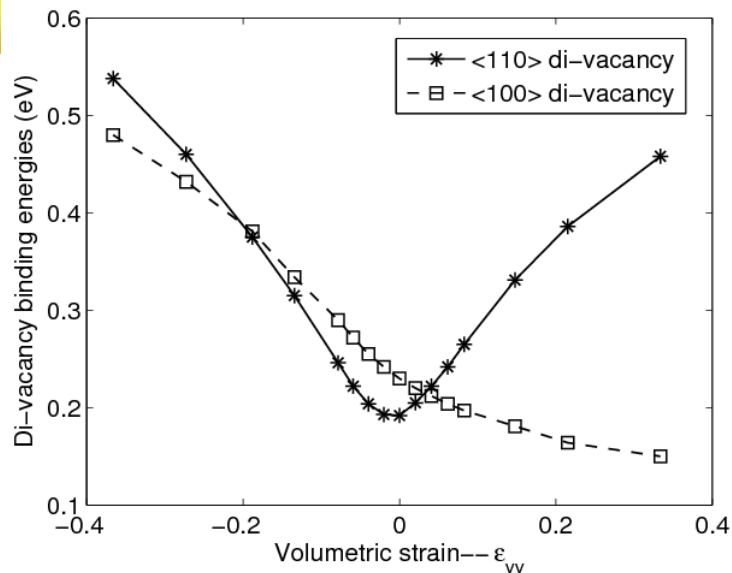
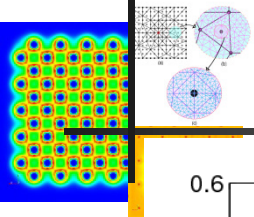
Role of macroscopic deformations on energetics of vacancies



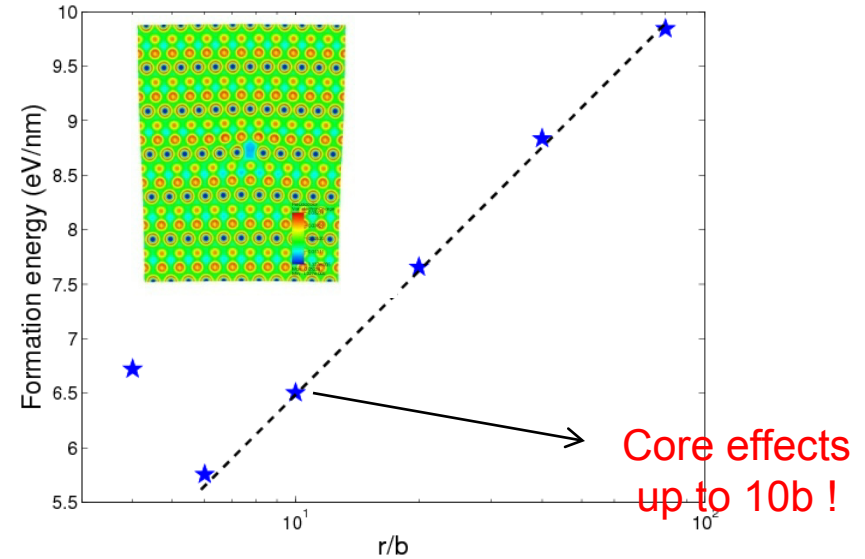
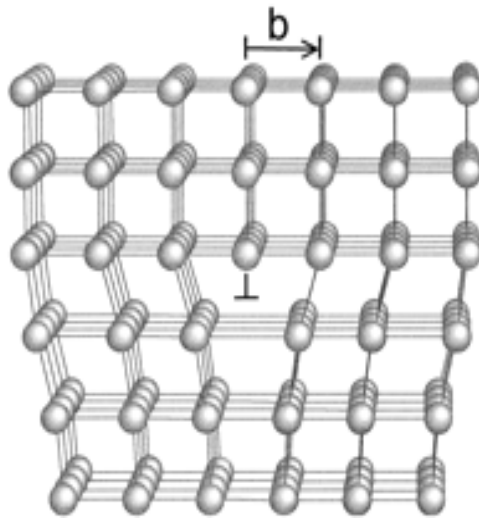
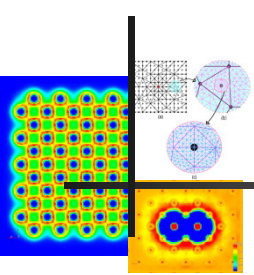
Universal dependence of formation energies on volumetric strain!



Role of macroscopic deformations on energetics of vacancies



Edge dislocation (in progress)



Incremental distance from the core	Elastic energy (eV/nm)	Electronic Relaxation (eV/nm)	Electronic Relaxation/Elastic energy (Absolute value)
$4b - 6b$	0.66254	-1.62796	2.457145
$6b - 10b$	0.869453	-0.12104	0.139211
$10b - 20b$	1.147981	0.004236	0.00369
$20b - 40b$	1.17937	-0.00061	0.000513
$40b - 80b$	1.066039	0.000403	0.000378



Kohn-Sham approach (KSDFT)

- Ground-state energy is a function of electron-density !! (Kohn & Sham, 1964-65)

$$\langle \psi | H | \psi \rangle \geq E_0 \quad (\text{Variational statement})$$

$$\begin{aligned} E_0 &= \min_{\psi} \langle \psi | T + \frac{1}{2} \sum_i' \sum_j' \frac{1}{|\mathbf{r}_i - \mathbf{r}_j|} + \sum_i V_{ext}(\mathbf{r}_i) | \psi \rangle + E_{zz} \\ &= \min_{\psi} \langle \psi | T + \frac{1}{2} \sum_i' \sum_j' \frac{1}{|\mathbf{r}_i - \mathbf{r}_j|} | \psi \rangle + \int \rho(\mathbf{r}) V_{ext}(\mathbf{r}) d\mathbf{r} + E_{zz} \\ &= \min_{\rho} \left\{ \underbrace{\left(\min_{\psi \rightarrow \rho} \langle \psi | T + \frac{1}{2} \sum_i' \sum_j' \frac{1}{|\mathbf{r}_i - \mathbf{r}_j|} | \psi \rangle \right)}_{F(\rho)} + \int \rho(\mathbf{r}) V_{ext}(\mathbf{r}) d\mathbf{r} \right\} + E_{zz} \end{aligned}$$

$$F(\rho) = T_s(\rho) + E_H(\rho) + E_{xc}(\rho) \longrightarrow \begin{array}{l} \text{Exchange-correlation} \\ \text{functional: Model using} \\ \text{LDA, GGA} \end{array}$$

↓
Kinetic energy of non-interacting electrons:
Computed from wave-functions of the resulting
E-L eqn.



Kohn-Sham approach (KSDFT)

➤ $E_0 = \min_{\rho \rightarrow N} \left\{ T_s(\rho) + E_H(\rho) + E_{xc}(\rho) + E_{ext} \right\} + E_{zz}$

➤ Consider the E-L equation corresponding to the variational problem:

$$\frac{\delta T_s}{\delta \rho} + \underbrace{V_H(\rho) + V_{xc}(\rho) + V_{ext}(\mathbf{R})}_{V_{eff}(\mathbf{r})} = \mu$$

$$\left(-\frac{1}{2} \nabla^2 + V_{eff} \right) \psi_i = \epsilon_i \psi_i$$

Self consistent iteration
(Kohn-Sham map)

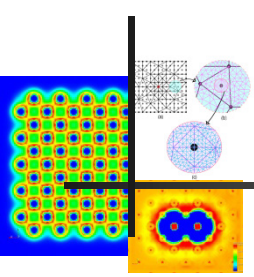
$$\rho = \sum_{i=1}^N |\psi_i|^2, \quad V_{eff}(\mathbf{r}) = V_H(\rho(\mathbf{r})) + V_{xc}(\rho(\mathbf{r})) + V_{ext}(\rho(\mathbf{r}))$$

$$T_s(\rho) = \frac{1}{2} \sum_{i=1}^N \int |\nabla \psi_i|^2$$

Kinetic energy computed
from the single electron
wave-functions



State of the art



Solutions to Kohn-Sham Equations

Fourier Space Formulations

Key Features

- Captures wide range of bulk properties
- Restrictive to periodic domains
- Provide only uniform spatial resolution
- Suitable when the solution fields are smooth.

Real Space Formulations (LCAO, FDM, FEM)

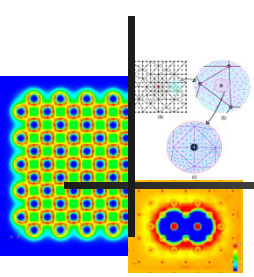
Key Features (FEM)

- Handle complex geometries and arbitrary boundary conditions
- Coarse Graining Capability
- Excellent Scalability of computations on massively parallel computing architectures

Though finite element basis is very versatile, number of basis functions in a linear finite element discretization required to achieve chemical accuracy is very large



Can higher-order finite-elements do any better?

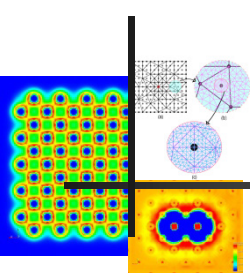


- Here, we investigate the viability and computational efficiency afforded by higher-order finite-element discretization in electronic structure calculations using density functional theory to answer the following questions:
 - ❖ What is the numerical convergence rate for various orders of finite-element approximations in electronic structure calculations using DFT?
 - ❖ What is the computational advantage derived by using higher-order finite element discretization in terms of the CPU time?

- We present some of the first studies which demonstrate the computational efficiency afforded by higher-order elements for Kohn-Sham DFT calculations.



Rate of convergence of the Finite Element Approximation



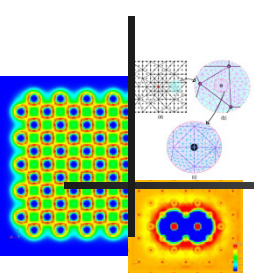
- The study has been carried out by a suite of higher order elements:
 - TET 10 (TETRAHEDRAL QUADRATIC ELEMENT)
 - HEX 27 (TRI QUADRATIC HEXAHEDRAL ELEMENT)
 - HEX 64 (TRI CUBIC HEXAHEDRAL ELEMENT)
 - HEX 125 (TRI QUARTIC HEXAHEDRAL ELEMENT)
 - HEX 64 SPECTRAL, HEX 125 SPECTRAL ... upto 10th order
(Lagrange Polynomials are constructed on Gauss-Lobatto Legendre Points for spectral elements)

- Elements have been tested against three types of problems: (a) CH₄ (b) Barium Cluster (35 atoms)
 - (a) CH₄ : An all electron calculation
 - (b) Barium Cluster: Pseudopotential calculation

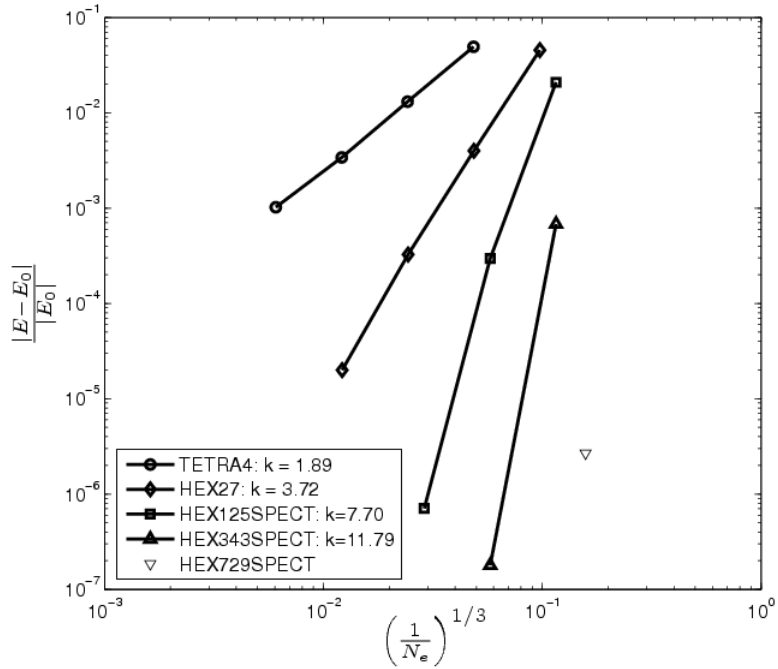


Convergence rates

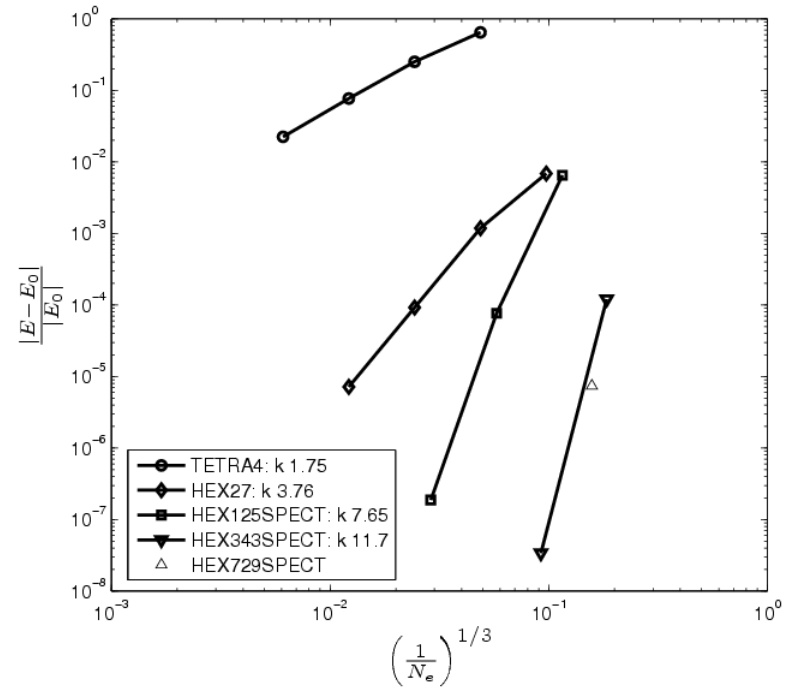
(Motamarri et al. J. Comp. Phys.)



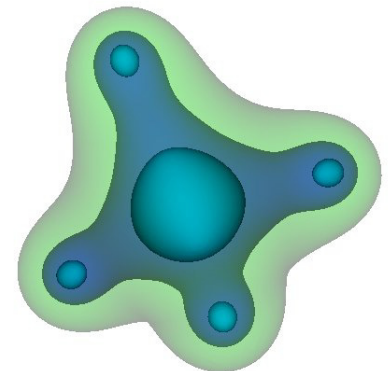
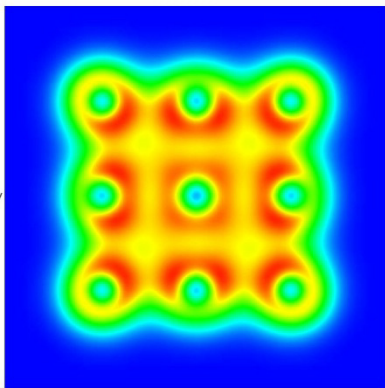
Barium Cluster



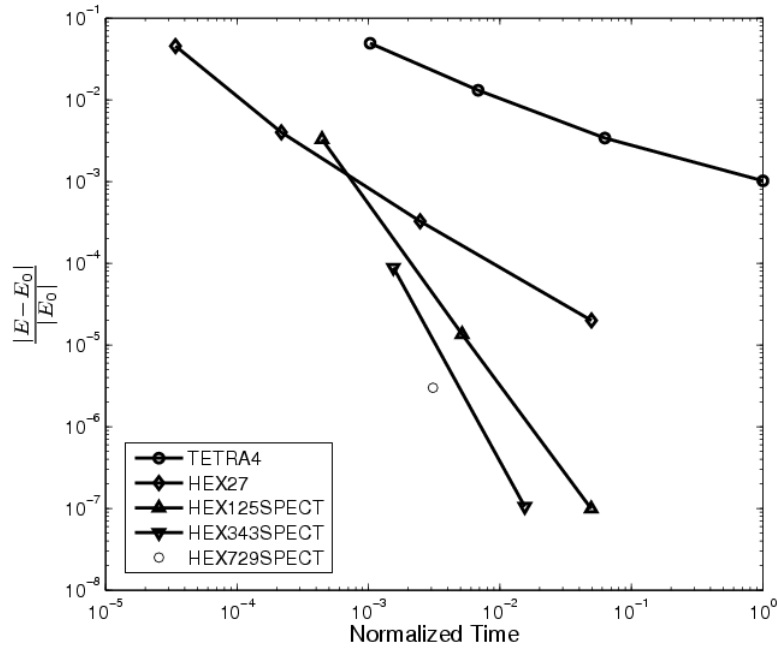
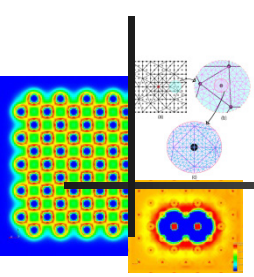
Methane Molecule



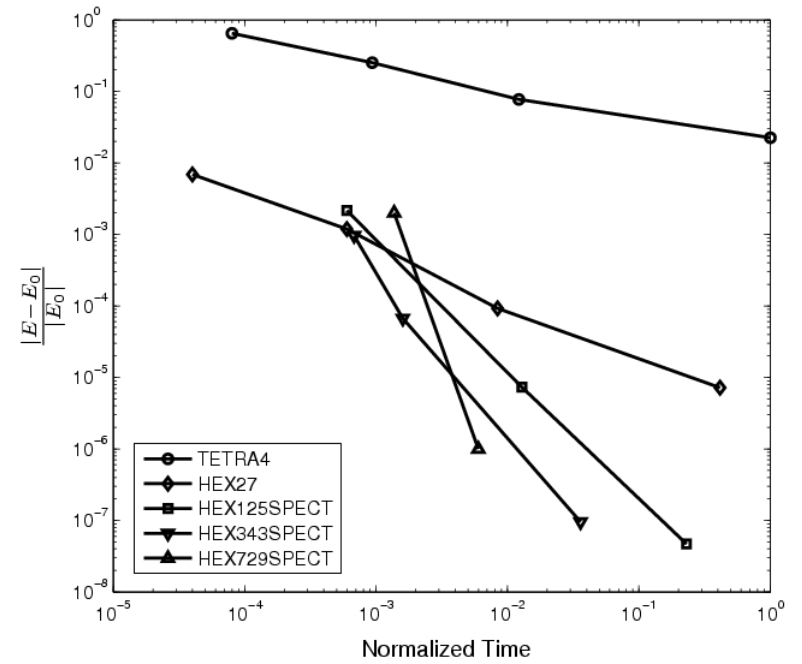
Optimal rate of convergence!



Computational efficiency



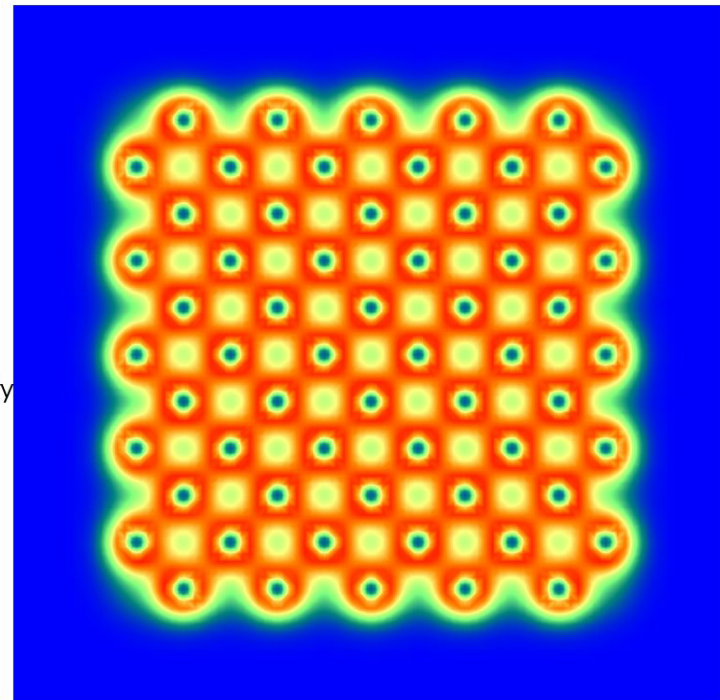
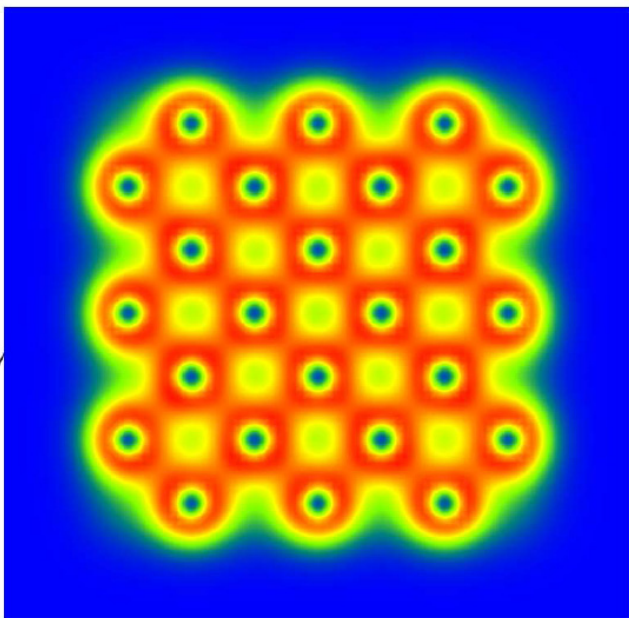
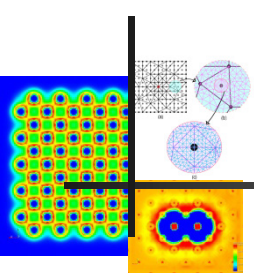
Barium Cluster



Methane Molecule



Aluminum clusters

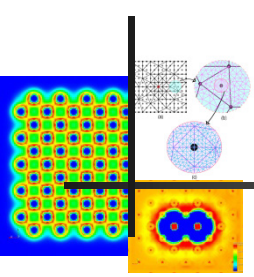


Type of basis set	Relative error	Time (CPU-hrs)
Plane-wave basis (cut-off 30 Ha , cell-size of 60 $a.u.$)	3.3×10^{-6}	646
FE basis (HEX343SPECT, 2,808,385 nodes, domain size: 200 $a.u.$)	3.6×10^{-6}	371

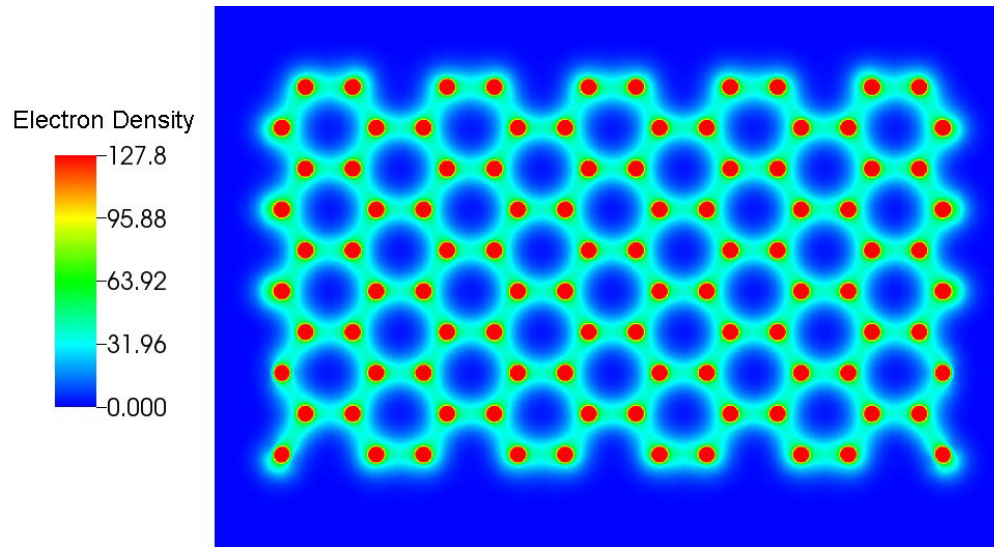
Type of basis set	Relative error	Time (CPU-hrs)
Plane-wave basis (cut-off 30 Ha , cell-size of 80 $a.u.$)	2.1×10^{-5}	7307
FE basis (HEX343SPECT, 7,875,037 nodes, domain size: 400 $a.u.$)	7.9×10^{-6}	6619



All-electron calculations



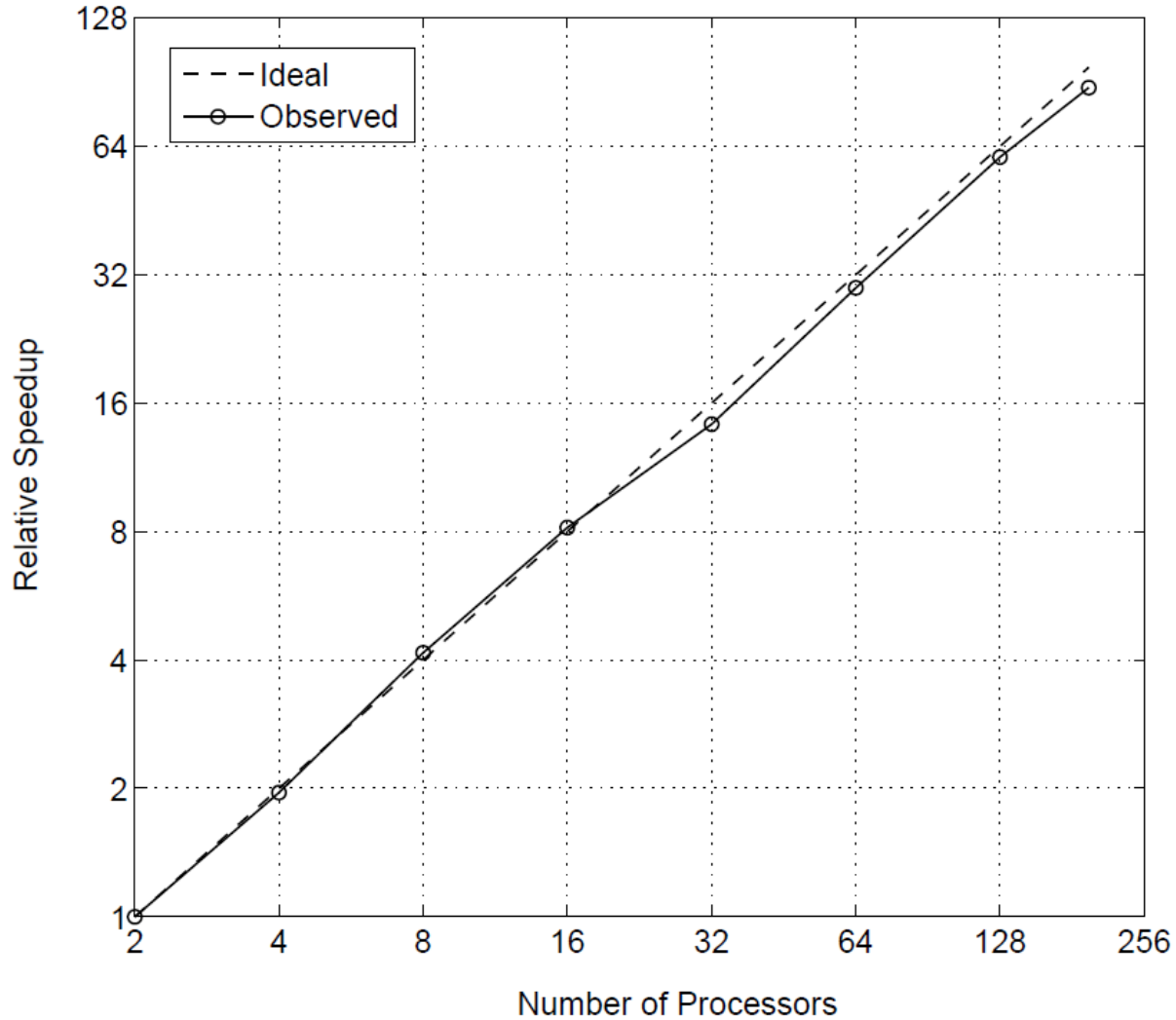
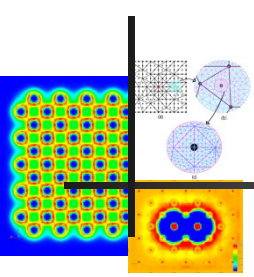
100 atom Graphene sheet

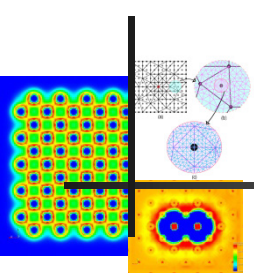


Type of basis set	Relative error	Time (CPU-hrs)
pc2 (Gaussian, 3,000 basis functions)	1.06×10^{-4}	666
FE basis (HEX125SPECT, 8,004,003 nodes)	1.2×10^{-4}	7461



Scalability





Ongoing/future work KSDFT

Real-space DFT-FE:

- Develop robust geometry optimization techniques
- Incorporate more advanced exchange-correlation functionals (beyond LDA, GGA)

Coarse-graining KSDFT:

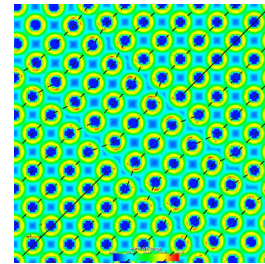
Localization of the wavefunctions is key for extending the coarse-graining ideas

- $O(N)$ formulations:
 - ❖ Non-orthogonal localized orbitals
(based on Garcia-Cervera et al. PRB 79 115110)
- QC-KSDFT: localization \rightarrow predictor-corrector approach \rightarrow QC
- Physical applications: electronic-structure informed study of deformation and failure mechanisms for structural materials; role of defects in electronic and optical properties; electron transport in open-systems

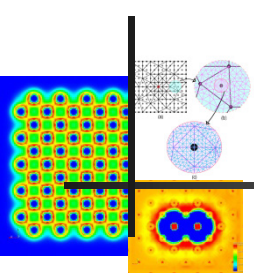


Concluding remarks

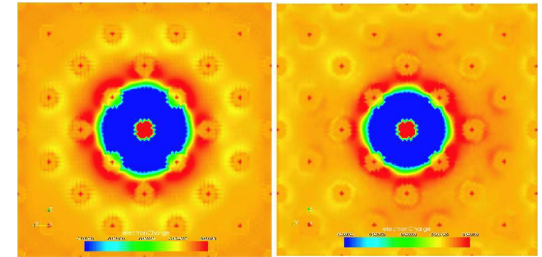
- Developed quasi-continuum orbital-free density-functional theory (QC-OFDFT)
 - ❖ Completely seamless and uses OFDFT as its sole input
 - ❖ Resolves the electronic structure of defect cores as well as macro-scale
 - ❖ Very important for accurate study of defects in materials
- The key ideas in QC-OFDFT are:
 - ❖ Real-space formulation of OFDFT
 - ❖ Finite-element discretization which is amenable unstructured coarse-graining
 - ❖ Predictor-corrector treatment of electronic fields; quadrature rules
- Study of vacancy clustering in aluminum through electronic structure calculations using QC-OFDFT
 - ❖ Vacancy clustering is energetically favorable
 - ❖ Vacancy clustering is a possible mechanism for prismatic loop formation



Concluding remarks



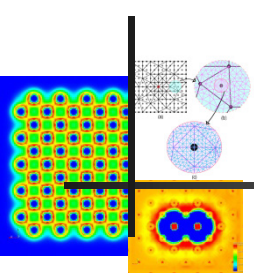
- Role of defect core in the energetics of defects
 - ❖ Influence of macroscopic deformation on the energetics of vacancies.
 - ❖ Multiple interacting length-scales
 - ❖ Volumetric strains have a dominant effect
- Real-space formulation KSDFT and finite-element discretization
 - ❖ Computational efficiency of higher-order FE
 - ❖ $O(N)$ formulation -> QC-KSDFT



References

- V. Gavini, J. Knap, K. Bhattacharya, M. Ortiz, Non-periodic finite-element formulation of orbital-free density-functional theory, *J. Mech. Phys. Solids* 55 669-696 (2007).
- V. Gavini, K. Bhattacharya, M. Ortiz, Quasi-continuum orbital-free density-functional theory: A route to multi-million atom DFT calculation, *J. Mech. Phys. Solids* 55 697-718 (2007).
- V. Gavini, K. Bhattacharya, M. Ortiz, Vacancy clustering and prismatic dislocation loop nucleation in aluminum, *Phys. Rev. B* 76 180101(R) (2007).
- V. Gavini, Role of macroscopic deformations on the energetics of vacancies, *Phys. Rev. Lett.* 101 205503 (2008).
- V. Gavini, Role of the defect core in energetics of vacancies, *Proc. Roy. Soc. A.* 465 3239-3266 (2009).
- B. Radhakrishnan, V. Gavini, Effect of the cell-size on the energetics of vacancies in aluminum studied via orbital-free density functional theory, *Phys. Rev. B* 82 094117 (2010).
- V. Gavini, L. Liu, A homogenization analysis of the field theoretic approach to the quasi-continuum method, *J. Mech. Phys. Solids* **59** 1536-1551 (2011).
- P. Mottamari, M. Iyer, J. Knap, V. Gavini, A higher-order adaptive finite-element discretization of orbital-free density functional theory, *J. Comp. Phys* **231** 6596-6621 (2012).
- P. Mottamari, M. R. Nowak, K. Leiter, J. Knap, V. Gavini, A higher-order adaptive finite-element discretization of orbital-free density functional theory, *J. Comp. Phys* (submitted).

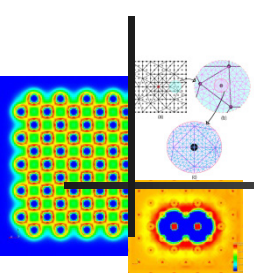




THANK YOU!



Configurational force (Eshelby tensor)



- Let $E_1(u_{eq}, \phi_{eq}, \mathbf{R}) = \min_u \max_\phi L(u, \phi, \mathbf{R})$
- Force on the I^{th} atom

$$\mathbf{f}_I = \frac{\partial E_1}{\partial \mathbf{R}_I} = \underbrace{\int_{\Omega} \frac{\partial b_I(\mathbf{r} - \mathbf{R}_I)}{\partial \mathbf{R}_I} \phi_{eq}}_{\text{Appears non-local}} = - \int_{\Omega} (\nabla b_I) \phi_{eq} = \underbrace{\int_{\Omega_c} (\nabla \phi_{eq}) b_I}_{\text{Infact, local}}$$

- Alternate expression:

Consider inner variations of the energy functional:

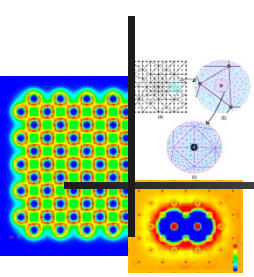
$\psi_\epsilon : \Omega \rightarrow \Omega'$, $\psi_0 = id$, $\Gamma = \left. \frac{d\psi_\epsilon}{d\epsilon} \right|_{\epsilon=0}$, such that $\Gamma = const$ in the compact support of b

$$\left. \frac{dE_1(\psi_\epsilon)}{d\epsilon} \right|_{\epsilon=0} = \int_{\Omega} \mathbf{E}_{ij} \frac{\partial \Gamma_i}{\partial y_j} dy, \quad \text{where}$$

$$\mathbf{E}_{ij} = L(u_{eq}, \phi_{eq}, \mathbf{R}) \delta_{ij} + \frac{1}{4\pi} \frac{\partial \phi}{\partial x_i} \frac{\partial \phi}{\partial x_j} - \lambda \frac{\partial u}{\partial x_i} \frac{\partial u}{\partial x_j}$$



OFDFT – Real-space formulation



- Electrostatic interactions can be re-written locally as,

$$E_H(u) + E_{ext}(u, \mathbf{R}) + E_{ZZ}(\mathbf{R}) =$$

$$- \inf_{\phi \in H^1(\mathbb{R}^3)} \left\{ \frac{1}{8\pi} \int |\nabla \phi(\mathbf{r})|^2 d\mathbf{r} - \int (u^2(\mathbf{r}) + b(\mathbf{r}; \mathbf{R})) \phi(\mathbf{r}) d\mathbf{r} \right\}$$

↓
(Regularized nuclear charges)

- Non-local kernel energies

$$T_k(u) = \int \int u^{2\alpha}(\mathbf{r}) K_{\alpha,\beta}(|\mathbf{r} - \mathbf{r}'|; u(\mathbf{r}), u(\mathbf{r}')) u^{2\beta}(\mathbf{r}') d\mathbf{r} d\mathbf{r}'$$

- Let

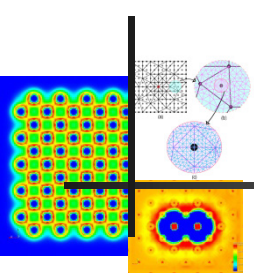
$$V_\alpha(\mathbf{r}) = \int K_{\alpha,\beta}(|\mathbf{r} - \mathbf{r}'|) u^{2\alpha}(\mathbf{r}') d\mathbf{r}', \quad \xrightarrow{\text{FT}} \quad \hat{V}_\alpha(\mathbf{k}) = \hat{K}_{\alpha,\beta}(\mathbf{k}) u^{\hat{2}\alpha}(\mathbf{k}),$$

$$V_\beta(\mathbf{r}) = \int K_{\alpha,\beta}(|\mathbf{r} - \mathbf{r}'|) u^{2\beta}(\mathbf{r}') d\mathbf{r}'. \quad \hat{V}_\beta(\mathbf{k}) = \hat{K}_{\alpha,\beta}(\mathbf{k}) u^{\hat{2}\beta}(\mathbf{k}).$$



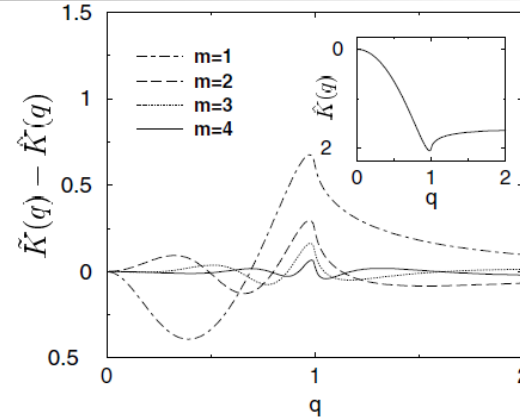
OFDFT – Real-space formulation (kernel energies)

(Radhakrishnan & Gavini PRB 2010)



$$\hat{K}_{\alpha,\beta}(\mathbf{k}) \approx \sum_{j=1}^m \frac{A_j |\mathbf{k}|^2}{|\mathbf{k}|^2 + B_j}$$

Choly & Kaxiras (2005)



➤ Local reformulation of kernel energy

$$V_{\alpha}(\mathbf{r}) = \sum_{j=1}^m [\omega_{\alpha_j}(\mathbf{r}) + A_j u^{2\alpha}(\mathbf{r})], \quad V_{\beta}(\mathbf{r}) = \sum_{j=1}^m [\omega_{\beta_j}(\mathbf{r}) + A_j u^{2\beta}(\mathbf{r})]$$

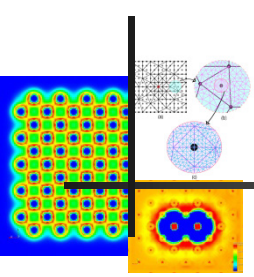
$$-\nabla^2 \omega_{\alpha_j} + B_j \omega_{\alpha_j} + A_j B_j u^{2\alpha} = 0, \quad -\nabla^2 \omega_{\beta_j} + B_j \omega_{\beta_j} + A_j B_j u^{2\beta} = 0 \quad j = 1 \dots m.$$

$$T_k(u) = \inf_{\omega_{\alpha_j} \in H^1(\mathbf{R}^3)} \sup_{\omega_{\beta_j} \in H^1(\mathbf{R}^3)} \sum_{j=1}^m \left\{ \int \left[\frac{1}{A_j B_j} \nabla \omega_{\alpha_j} \cdot \nabla \omega_{\beta_j} + \frac{1}{A_j} \omega_{\alpha_j} \omega_{\beta_j} + \omega_{\beta_j} u^{2\alpha} + \omega_{\alpha_j} u^{2\beta} + A_j u^{2(\alpha+\beta)} \right] d\mathbf{r} \right\}.$$

Local saddle point problem in kernel potentials



OFDFT – Real-space formulation



- The saddle-point problem is given by,

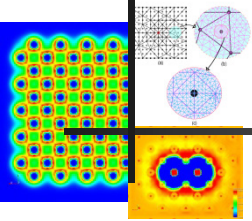
$$\inf_{\mathbf{R} \in \mathbf{R}^{3M}} \inf_{u \in H^1(\mathbf{R}^3)} \sup_{\phi \in H^1(\mathbf{R}^3)} \inf_{\omega_{\alpha_j} \in H^1(\mathbf{R}^3)} \sup_{\omega_{\beta_j} \in H^1(\mathbf{R}^3)} L(u, \mathbf{R}, \phi, \omega_{\alpha_j}, \omega_{\beta_j}) \quad \text{subject to: } \int u^2(\mathbf{r}) d\mathbf{r} = N$$

$$\begin{aligned} L(u, \mathbf{R}, \phi) = & \int \left[\frac{1}{2} |\nabla u|^2 + C_F u^{10/3} + \varepsilon_{xc}(u^2) u^2 - \frac{1}{8\pi} |\nabla \phi|^2 + (u^2 + b(\cdot; \mathbf{R})) \phi \right. \\ & \left. + \sum_{j=1}^m \left(\frac{1}{A_j B_j} \nabla \omega_{\alpha_j} \cdot \nabla \omega_{\beta_j} + \frac{1}{A_j} \omega_{\alpha_j} \omega_{\beta_j} + \omega_{\beta_j} u^{2\alpha} + \omega_{\alpha_j} u^{2\beta} + A_j u^{2(\alpha+\beta)} \right) \right] d\mathbf{r} \end{aligned}$$

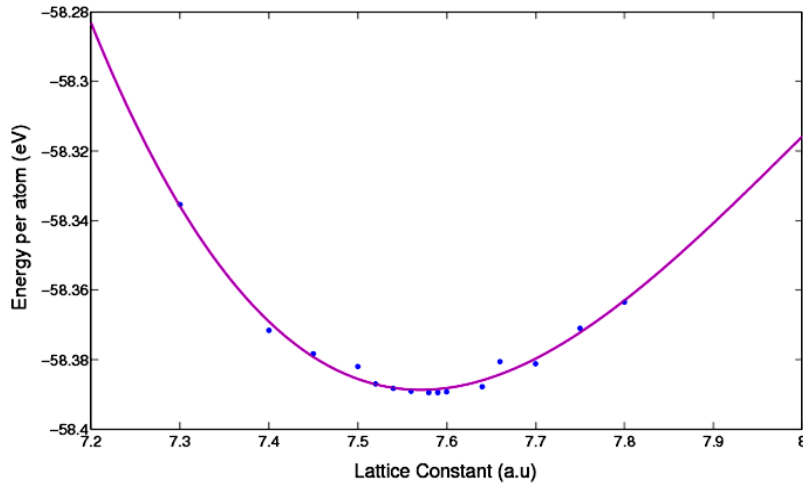
- Well-posedness is an open question! (Blanc & Cancès 2005)



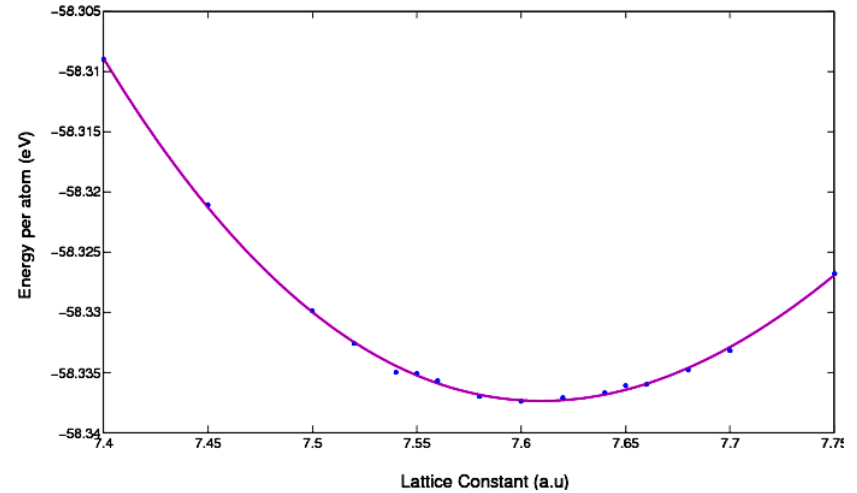
Bulk properties of Aluminum



Density Independent Kernels



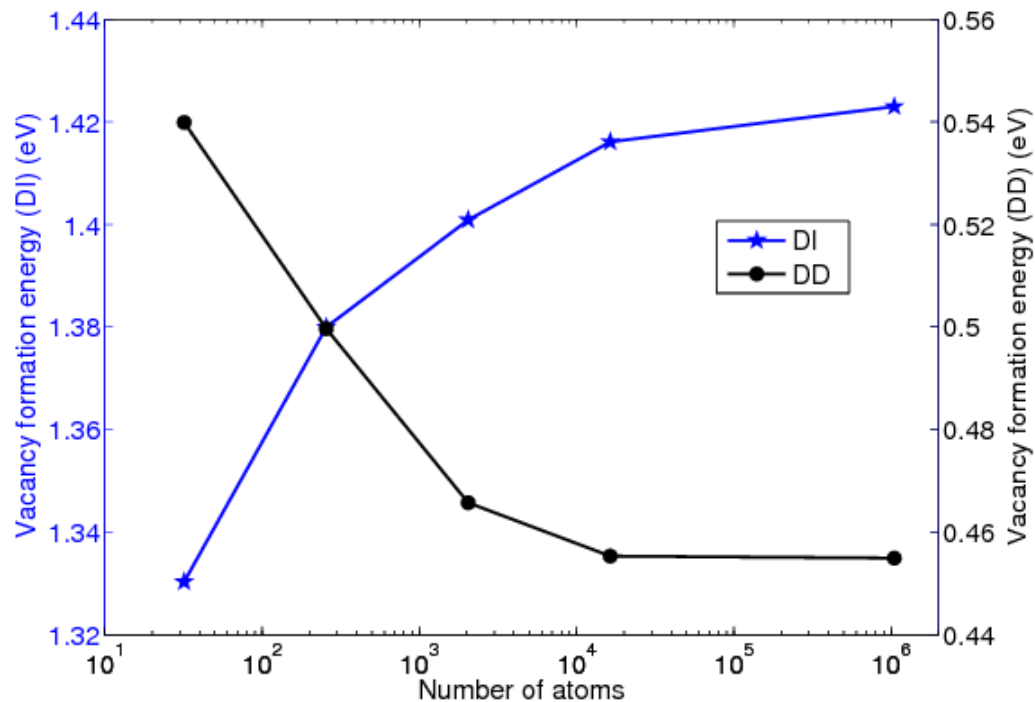
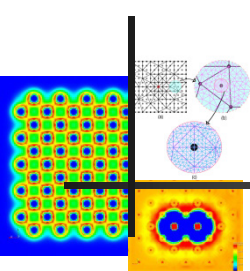
Density Dependent Kernels



	KS-DFT (Goodwin et. al.)	Gavini et al. (TF-vW)	Carter et. al. (Density Independent)	OFDFT (Density Independent)	Carter et al. (Density Dependent)	OFDFT (Density Dependent)
Bulk Modulus (GPa)	79	83.1	71.9	72	72	71.72
Energy per atom (eV)	-58.336	-58.81	-58.334	-58.3895	-58.331	-58.3374
Eq. lattice Const.	7.44	7.42	7.59	7.58	7.61	7.6



Vacancy in Aluminum: Convergence with cell-size



Domain size (No. of atoms + 1 vacancy)	Vacancy formation energy (eV)					
	OFDFT (Density Independent)	Carter et. al (Density Independent)	OFDFT (Density Dependent)	Carter et. al (Density Dependent)	Exp.	Gavini et.al (TFW- λ)
32	1.33	1.35	0.5399	0.512	0.66	0.77
256	1.38	-NA-	0.4993	0.475	0.66	0.74



Di-vacancy binding energy – cell-size effect

